Dynamics of macrophage polarization reveal new mechanism to inhibit NLRP-3 inflammasome and IL-1β release via extracellular ATP and pyrophosphates

Pablo Pelegrin[1,2] and Annmarie Surprenant[1]

[1]Faculty of Life Sciences, Michael Smith Building, University of Manchester

Manchester M13 9PT, United Kingdom

[2]Present address: Inflammation and Experimental Surgery Group. University Hospital "Virgen de la Arrixaca"-FFIS, Murcia, Spain.

Correspondence authors: **P Pelegrin**, Inflammation and Experimental Surgery Group. University Hospital "Virgen de la Arrixaca"-Fundación Formación e Investigación Sanitarias Región de Murcia (FFIS), 30120 El Palmar, Murcia, Spain; pablo.pelegrin@ffis.es. Phone: 34-968369317; Fax: 34-968369368; **A Surprenant**, Faculty of Life Science, Michael Smith Building D3315, University of Manchester, Manchester M13 9PT UK. a.surprenant@manchester.ac.uk. Phone: 44-1613060505; Fax: 44-1612751498 (**A Surprenant for editorial contact**).

Running title: Actin clustering prevents inflammasome activation

Key words: NLRP-3 inflammasome, alternative macrophage activation, $P2X_7$ receptor, caspase-1, inflammation

Total characters = 53,748 including spaces

ABSTRACT

In acute inflammation extracellular ATP activates $P2X_7$ ion channel receptors ($P2X_7R$) on M1 polarized macrophages to release pro-inflammatory IL-1β via activation of the caspase-1/Nucleotide-binding domain and Leucine-rich repeat receptor containing Pyrin domain 3 (NLRP3) inflammasome. In contrast, M2 polarized macrophages are critical to the resolution of inflammation but neither actions of $P2X_7R$ on these macrophages, nor mechanisms by which macrophages switch from pro-inflammatory to anti-inflammatory phenotypes, are known. Here we investigated extracellular ATP signaling over a dynamic macrophage polarity gradient from M1 through M2 phenotypes. In macrophages polarized towards, but not at, M2 phenotype, where intracellular IL-1β remains high and the inflammasome is intact, $P2X_7R$ activation selectively uncouples to the NLRP3-inflammasome activation but not to upstream ion channel activation. In these intermediate M1/M2 polarized macrophages, extracellular ATP now acts via its pyrophosphate chains, independently of other purine receptors, to inhibit IL-1β release by other stimuli via two independent mechanisms: inhibition of ROS production and trapping of the inflammasome complex via intracellular clustering of actin filaments.

INTRODUCTION

Macrophages are critical to both the innate and adaptive immune response; they must develop and respond to rapid changes in the microenvironment. Inflammation resulting from pathogens or tissue damage activates resident macrophages to initiate or increase production of pro-inflammatory cytokines and other inflammatory mediators. However, macrophages are equally critical in the resolution of inflammation by producing anti-inflammatory cytokines and chemokines and by increased phagocytic activity. Based on Th1/Th2 polarization concepts (Romagnani, 2000), phenotypically polarized macrophages are now generally termed pro-inflammatory M1, or classically activated, and anti-inflammatory M2, or alternatively activated (Gordon, 2003; Martinez et al., 2008). Experimentally, macrophages *in vitro* are polarized to the M1 state by treatment with IFN-γ and inducers of TNF-α, such as lipopolysaccharide (LPS) or other bacterial products (Ehrt et al., 2001; Gordon, 2003). M1 macrophages induce synthesis and upregulation of several pro-inflammatory cytokines and chemokines, key among these are TNF–α, IL-12, IL-6, CCL2 and IL-1β, as well as increased production of reactive oxygen (ROS) and nitrogen intermediates (Gordon, 2003; Martinez et al., 2008). At the other extreme, macrophages are polarized to the M2 state by stimuli such as IL-4, IL-13, IL-10 or glucocorticoid hormones (Gordon, 2003; Martinez et al., 2008). M2 macrophages upregulate scavenger, mannose and galactose receptors, IL-1 receptor antagonist and downregulate IL-1β and other pro-inflammatory cytokines (Gordon, 2003; Scotton et al., 2005; Martinez et al., 2006; 2008). Very high levels of IL-1β are present in M1 polarized macrophages due to activation of the NF-κB and MAPK cascades (Dinarello, 1996) but no IL-1β protein is found in M2 polarized macrophages (Scotton et al., 2005; Martinez et al., 2006).

IL-1β processing and release is a tightly regulated process involving a multiprotein complex, the capase-1 inflammasome (Martinon et al., 2002). IL-1β is synthesized as a 34 kD precursor protein that is cleaved to its biologically active 17 kD form by the protease caspase-1. Inactive caspase-1 is constitutively present in both M1 and M2 macrophages and is activated in M1 macrophages by self-cleavage that occurs in the inflammasome complex. Distinct caspase-1 inflammasomes have been distinguished based on their protein composition and means of activation

(Kanneganti et al., 2006; Mariathasan et al., 2004; 2006; Martinon et al., 2006). The nucleotide-binding domain and leucine-rich repeat receptor containing pyrin domain 3 (NLRP3)-inflammasome can be activated by specific microbial motifs (pathogen-associated molecular patterns, PAMPs), by *Escherichia coli* and *Staphylococcus aureus* bacteria, by microbial toxins such as nigericin and maitotoxin (MTX), by uric acid crystals, and by extracellular ATP acting via the ATP-gated plasma membrane ion channel, the $P2X_7$ receptor ($P2X_7R$) (Mariathasan et al., 2004; 2006; Martinon et al., 2006; Petrilli et al., 2007). $P2X_7R$ activation by ATP released at sites of inflammation is currently the only well established physiological stimulator of the NLRP3 inflammasome (Mariathasan et al., 2004; 2006; Ferrari et al., 2006) and, as such, it has become an attractive target for development of new anti-inflammatory drugs (Pelegrin, 2008). $P2X_7R$ gene deleted mice show anti-inflammatory phenotypes in models of neuropathic and inflammatory pain (Labasi et al., 2002; Chessell et al., 2005) and a recently developed $P2X_7R$ antagonist has shown reduced joint swelling, tenderness and pain perception in Phase II clinical trails in patients with rheumatoid arthritis (McInnes et al., 2007). The $P2X_7R$ is a highly unusual ion channel predominantly expressed in macrophage and microglia; its activation opens a cationic channel with high permeability to calcium but it also forms within seconds a larger pore permeable to small molecules up to 900 dalton (Ferrari et al. 2006; Pelegrin and Surprenant, 2006). All downstream sequelae of $P2X_7R$ activation except for the initial cation channel opening require the presence of the intracellular C-terminus which is key to the formation of the $P2X_7R$-multiprotein complex (Ferrari et al. 2006).

The present study was prompted by a surprising observation we made while comparing *E. coli* and $P2X_7R$-induced activation of the NLRP3 inflammasome and IL-1β release in M1 polarized macrophages. We found that, while *E. coli*-induced release of IL-1β remained constant, ATP-evoked IL-1β release ceased over time in spite of continued high levels of intracellular IL-1β and without decreased functional $P2X_7R$ as assayed by upstream ion channel signaling. We found that unexpected changes in the polarization state of the macrophages were causing a $P2X_7R$-specific uncoupling to the caspase-1 cascade. We therefore developed an *in vitro* model of a likely macrophage polarization gradient from extreme M1 through to extreme M2 and examined the actions of different NLRP3 inflammasome activators (ATP, *E. coli*,

maitotoxin and nigericin) over this polarization gradient, as well as in acute and chronically $P2X_7R$-deleted M1 polarized macrophages. This study has identified a new mechanism by which extracellular ATP produces physiological inhibition of IL-1β release that may be key to switching a macrophage from an inducer of inflammation toward its anti-inflammatory phenotype in the resolution phase of infection or inflammation.

RESULTS

Characterization of a dynamic macrophage polarity gradient

We developed an *in vitro* polarization protocol designed to rapidly mimic (over 4 – 8 h) a continuum of signals that are likely to drive the macrophage from the classic inflammatory M1 polarity to the anti-inflammatory M2 state (Figure S1A available online). Macrophages from polarities close to M1 (states 1 – 3) were expanded and tightly fixed to substrate, formed numerous lamellar processes and elongated filopodia, with diffuse F-actin staining throughout the cytoplasm but distinctly absent from the filopodia (Figure 1A,B). Macrophages from a polarity close to M2 (state 4) presented less lamellar processes but remained expanded and tightly fixed to the substrate while the extreme M2 polarized (alternatively activated) macrophages had the same morphology as untreated cells with F-actin being tightly compacted close to the nucleus (Figure 1A,B). We quantified these changes in cell morphology by measuring total surface area over all polarizations states and found a gradual progression from M1 through M5 states (Figure 1C; n = 50-70 for each polarization state). We also confirmed that our protocols did, indeed, establish a molecular polarization gradient by quantitative RT-PCR (qPCR) for the classical M1 and M2 genes, TNFα and mannose receptor C (MRC-1) (Gordon, 2003; Martinez et al., 2008); TNFα gene expression was upregulated by 200-fold in M1 macrophages and this gradually decreased to near zero in extreme M2 macrophages while MRC-1 gene expression gradually increased over the gradient to reach a 10-fold upregulation at extreme M2 polarization (Figure 1D).

$P2X_7R$, but not *E. coli*, uncouples to inflammasome activation during macrophage polarization

We found that intracellular levels of proIL-1β remained high in all polarization states (1 – 4) except, as expected (Gordon, 2003; Martinez et al., 2008), the alternatively activated M2 macrophages (Figure 2A,B). ATP stimulation of $P2X_7R$ in M1 activated macrophage, or *E. coli* infection are both well characterized pathways known to initiate NLRP3-inflammasome dependent release of mature IL-1β (Ferrari et al., 2006; Mariathasan et al., 2006; Petrilli et al., 2007). However, we found striking differences in their ability to release IL-1β over the polarization gradient. In

agreement with numerous studies (Mariathasan et al., 2006; Pelegrin and Surprenant, 2006; 2007; Petrilli et al., 2007), both $P2X_7R$ and *E. coli* stimulation induced the release of IL-1β from M1 polarized macrophages but $P2X_7R$-induced release of IL-1β was significantly reduced, or absent, in macrophages of intermediate polarity (states 3,4; Figure 2A,B). Conversely, *E. coli* induced significantly greater IL-1β release from these intermediately polarized macrophages (Figure 2B). Moreover, we observed a similar uncoupling of $P2X_7R$ from IL-1β release during traditional long-term activation of macrophages with LPS/IFNγ (Arend et al., 1989). That is, while $P2X_7R$ or *E. coli* –induced release of IL-1β peaked at similar times (5-10 h post activation with either LPS/IFNγ or *E. coli*), ATP failed to stimulate IL-1β release subsequently in spite of maintained high levels of intracellular IL-1β and in contrast to the continued release of IL-1β by *E. coli* (Figure 2C). Initially we hypothesized a decrease in $P2X_7R$ expression was the most likely explanation for the failure of ATP to stimulate IL-1β release under these conditions, as clearly the NLRP3-inflammasome cascade known to be activated by *E. coli* (Petrilli et al., 2007) was not affected. However, we could not attribute this loss of $P2X_7R$-mediated release of IL-1β to loss of functional receptors because: (i) $P2X_7R$ gene expression was actually down-regulated in M1 macrophages and did not change from states 1 – 3, then increased in state 4 and 5 (Figure 1D); (ii) $P2X_7R$ protein localization remained constant through all polarization states, in particular the $P2X_7R$ protein showed a similar punctate expression along the cell (Figure 2D), (iii) assays for upstream signalling of $P2X_7R$ (calcium flux and dye-uptake) (Pelegrin and Surprenant, 2006) did not change over the polarity gradient (Figure 2E,F). Macrophages obtained from $P2X_7R$-gene deleted mice were subjected to the same polarization gradient protocols and served as controls; in these macrophage no anti-$P2X_7R$ antibody staining was present (data not shown) and no ATP-mediated calcium flux or dye-uptake occurred in M1 macrophages (Figure 2E,F) or in M2 macrophages (data not shown).

From positive to negative regulation of IL-1β release by ATP during macrophage polarization

We next compared inflammasome activation profiles induced by ATP and by two toxins, maitotoxin (MTX) and nigericin, which activate the NRLP3-inflammasome with similar kinetics and mechanisms to $P2X_7R$ but which are not dependent on $P2X_7R$ (Mariathasan et al., 2006; Pelegrin and Surprenant, 2007) (Figure S1B). IL-1β ELISA assays (which recognize pro and mature forms of the cytokine) revealed that ATP-induced release of IL-1β was reduced by 50 – 80% in state 3 intermediate polarized macrophages compared to M1 polarized cells (Figure 2B and 3A) while MTX-induced IL-1β release was the same in macrophages from either polarity state and similar to levels of ATP-induced release from M1 macrophages (Figure 3A). When ATP and MTX were co-applied, IL-1β release was increased in M1 macrophages to the same extent as in the presence of either compound alone (Figure 3A). However, co-application of MTX and ATP to state 3 polarized macrophages resulted in a 50% reduction of IL-1β release (Figure 3A). Western blots showed typical release of mature IL-1β from M1 macrophage in response to ATP, MTX or a combination of MTX and ATP while in state 3 polarized macrophages, mature IL-1β was detected in response to MTX but not ATP stimulation and co-application significantly decreased release of mature IL-1β (Figure S2A). Strikingly, ATP completely prevented MTX-induced release of IL-1β in M1 polarized macrophages after acute blockade of $P2X_7R$ with the $P2X_7R$-selective antagonist, A740003 (Honore et al., 2006) (Figure 3B and S2B). ATP similarly inhibited both MTX and nigericin-induced release of IL-1β from M1 polarized macrophages obtained from $P2X_7R$-deleted mice (Figure 3C and S2C). ATP also inhibited caspase-1 activation (Figure 3C, lower panels) and release of the inflammasome adaptor protein, Apoptosis-associated Speck-like protein containing a C-terminal Caspase-activating recruiting domain (ASC, Figure 3D) induced by either MTX or nigericin in M1 polarized $P2X_7R^{-/-}$ macrophages. Re-introduction of $P2X_7R$ into $P2X_7R^{-/-}$ macrophages via adenoviral delivery reconstituted all features of ATP-mediated IL-1β release and caspase-1 activation from M1 polarized macrophages (Figure S1D,E). ATP also failed to induce caspase-1 activation in M2 wildtype polarized macrophages (Figure 3E), although upstream signalling via $P2X_7R$ (calcium flux, dye-uptake) were not significantly different than observed in M1 macrophages. Taken together, these results show that the inhibitory action of ATP on these macrophages was due solely to lack of $P2X_7R$ downstream signalling and not to alterations in the NLRP3

inflammasome itself. ATP was equally able to inhibit IL-1β release from the *in vitro E. coli* model of infection and slow NLRP3 activation (e.g. Figure 2C and S1C) in M1 polarized macrophages from $P2X_7R^{-/-}$ macrophages (Figure 3F and S2D). This inhibition was not due to alterations in binding or phagocytosis of the bacteria by these macrophages in the presence of ATP (Figure S2E).

Negative regulation of IL-1β by ATP is not via purinoreceptors but is due to pyrophosphate actions

We expected the inhibitory actions of ATP which occurred during macrophage polarization from M1 towards M2 states, or which were revealed by acute (selective $P2X_7R$ antagonist) or chronic ($P2X_7R^{-/-}$ macrophage) blockade of $P2X_7R$, to result from activation of one, or more, purinergic P2X, P2Y or adenosine receptors. However, results shown in Figures 4, S3A, and S3E quickly ruled out involvement of any of these receptors in the inhibition of IL-1β release by ATP. We used M1 polarized macrophages from $P2X_7R^{-/-}$ mice (Figure 4A-E) or from wildtype mice in the presence of A740003 (data not shown) and examined the actions of ATP and other purines on MTX-induced IL-1β release and caspase-1 activation. Firstly, the ATP concentration-inhibition curve was 20 – 100-fold to the right of all known purine and adenosine receptors except for $P2X_7R$; indeed, the IC_{50} value for ATP inhibition of MTX-induced IL-1β release in $P2X_7R$ depleted macrophage (1.54 ± 0.03 mM, n = 3) was not significantly different from the ATP EC_{50} value to induce release of IL-1β from wildtype M1 macrophages (1.65 ± 0.02 mM, n = 3) (Figure 4A,E). Secondly, significant inhibition was observed with ATP > ADP >> AMP but not with adenosine (Figure 4B,C). Thirdly, the non-selective P2X/P2Y inhibitor, suramin, and the non-selective P2X antagonist, PPADS, did not alter the inhibition by ATP of the nigericin-induced IL-1β in $P2X_7R$-deficient M1 macrophages (Figure S3A). Most directly, pyrophosphate (PPi, Figure 4B-E) and triphosphate (Figure S3C) but not monophosphate (Figure 4D) inhibited IL-1β release and caspase-1 activation more potently than ATP, with an IC_{50} value for PPi of 1.03 ± 0.05 mM (n = 3). The non-hydrolyzable bisphosphonate, clodronate (Figure S3D), exerted the same inhibition and was 3-5-fold more potent than PPi or ATP, with an IC_{50} value of 0.43 ± 0.14 mM. (Figure 4D,E). Both PPi and clodronate were effective to inhibit MTX-mediated IL-

1β release from wildtype M1 or M1/M2 intermediate polarized macrophages but neither inhibited ATP-mediated release from these cells (Figure 4F). Finally, in HEK cells heterologously expressing P2X receptors or endogenously expressing P2Y receptors, neither PPi (5 mM) nor clodronate (1 mM) alone had any effect on membrane currents (data not shown) or cytosolic calcium transients, and nor did they significantly alter the ATP-evoked responses in these cells (Figure S3E).

Clodronate, and other bisphosphonates, when encapsulated in liposomes, have been a widely used mechanism to selectively destroy macrophages (van Rooijen and Sanders, 1994) because macrophages phagocytose the liposomes, lysosomal phospholipases break down the liposomes and the resulting free intracellular bisphosphonates initiate apoptosis (van Rooijen and Sanders, 1997). Free bisphosphonates have not been found to accumulate intracellularly (Pennanen et al., 1995). Nevertheless, we asked whether the application of clodronate as used in our experiments (up to 30 min applications) may have toxic actions on macrophage that would explain the inhibition of IL-1β by measuring LDH release from all experiments (Figure S3B). No increase in LDH release over basal conditions was observed and in all cases LDH release was < 1-3% of total LDH levels (n = 10-14). This result, and the observation that clodronate alone did not alter intracellular calcium levels (Figure S3E), provide conclusive evidence against a toxic action of clodronate on these macrophages.

ATP differentially regulates actin polymerization and inflammasome localization during macrophage polarization gradient

$P2X_7R$ and MTX stimulation of M1 polarized macrophages are associated with rapid and dramatic cytoskeletal re-arrangements (Pfeiffer et al., 2004; Verhoef et al., 2004). We noticed a striking difference in the actions of ATP on cell morphology over the M1 to M2 polarization gradient, and therefore asked whether this may be associated with their actions to inhibit inflammasome activation. We examined F-actin distribution before, and 5 min after the addition of ATP (5 mM), MTX (0.2 nM) or ATP with MTX, in M1 polarized wildtype and $P2X_7R^{-/-}$ macrophage, in intermediate state 3 polarized wildtype macrophage, and in M1 polarized wildtype macrophage

treated with A740003 (Figure 5A). ATP induced intense F-actin distribution to only one side of the cell with extensive ramifications radiating outward over the other side; MTX induced an equally intense but uniform F-actin localization around the entire cell while co-application produced a randomly radiating network of F-actin (Figure 5A, panels i-iv and S4C). In striking contrast, ATP induced an intense intracellular clustering of F-actin in macrophage from intermediate state 3 polarization as well as from acute and chronic $P2X_7R$-depleted macrophages (Figure 5A, panels vi,x,xiv) while MTX produced essentially the same F-actin pattern as observed in M1 polarized wildtype macrophages (Figure 5A, panels vii,xi,xv). Co-application of ATP and MTX to intermediate state 3 polarized macrophages produced both intracellular F-actin clustering and radiating F-actin ramifications (Figure 5A, panel viii) but co-application to $P2X_7R$-depleted M1 macrophages produced the same pattern of intense intracellular clustering as seen with ATP alone in these macrophages (Figure 5A, panel xii and S4C). PPi and clodronate induced a similar pattern of intracellular clustering of F-actin when co-applied with MTX in $P2X_7R$-depleted macrophages and prevented polymerization of F-actin to the cell edge (Figure S4A and S4C).

To investigate whether the dynamics of F-actin polymerization were important for the inhibition of inflammasome activation by ATP and PPi, we treated M1 polarized $P2X_7R^{-/-}$ macrophages with cytochalasin B (CB) to disrupt coordinated actin cytoskeleton assembly. In agreement with previous studies demonstrating that actin-based cytoskeletal pathways are not directly involved with IL-1β processing and release (Hornung et al., 2008), we found that CB itself did not induce IL-1β release nor did it alter MTX-induced release (Figure 5B,C). However, CB partially reversed (by 30 – 50%) the blockade of MTX-induced IL-1β by ATP and PPi (Figure 5B,C) and prevented intracellular actin clustering (Figure S4B). To gain further insight into potential mechanisms underlying this previously undetected involvement of the actin cytoskeleton in NLRP3-inflammasome inhibition, we used a caspase-1 specific fluorescent probe to directly identify active caspase-1 within the macrophage. No active caspase-1 was detected in unstimulated M1 polarized macrophages from $P2X_7R^{+/+}$ (Figure 6A, upper panels) or $P2X_7R^{-/-}$ mice (Figure 6B, left panel). Stimulation of M1 polarized wildtype macrophages with ATP, or $P2X_7R^{-/-}$ macrophages with MTX, for 5 min led to robust caspase-1 activation in discrete intracellular aggregates that are likely to represent sites of active inflammasome

complexes (Figure 6A, lower panels and 6B, middle panel). Several of these active caspase-1 aggregates were observed within the actin barrier at the edge of the cell (Figure 6A,B, arrows), suggestive of potential caspase-1/IL-1β release sites. ASC immunostaining of unstimulated M1 macrophages showed a uniform cytosolic distribution (Figure 6A, upper middle panel), while ASC formed clusters after ATP stimulation, many of which co-localized with active caspase-1 (Figure 6A, arrowheads), confirming their status as an activated inflammasome complex. However, we also observed many ASC-only and caspase-1-only aggregates upon ATP stimulation which may indicate heterogeneous subpopulations of inflammasome-like complexes (Figure 6A, lower middle panel). We did not observe any co-localization of active caspase-1 with the lysosomal marker, cathepsin L (Figure 6A, right panels), which is in agreement with recent studies showing that the early release of IL-β does not occur via lysosomal secretory pathways (Brough and Rothwell, 2007).

Modulation of redox signalling by ATP and PPi during macrophage polarization

We hypothesized that the inhibition of IL-1β processing and release by ATP and PPi that was not reversed by treatment with CB (i.e. the actin-independent inhibition) may result from reduced reactive oxygen species (ROS) production because $P2X_7R$ stimulation of M1 polarized macrophages is known to increase ROS production, is associated with NLRP3 inflammasome activation (Dostert et al., 2008; Hewinson et al., 2008) (Figure S4D) and ATP, PPi and bisphosphonates may act directly or indirectly as oxygen radical scavengers (Serretti et al., 1993; Kachur et al., 1997; Dombrecht et al., 2006). Both ATP and MTX induced similar rapid (within 2-3 min) increases in ROS production from M1 polarized macrophages (Figure 7A,E) but in M2 polarized macrophages the enhanced ROS production was significantly delayed (no significant increase occurred before 8 – 10 min) and reduced (Figure 7B,E). MTX similarly increased ROS production from M1 polarized $P2X_7R^{-/-}$ macrophages (Figure 7C,E), but MTX-induced ROS production in these cells was prevented by ATP, PPi and clodronate with IC_{50} values not significantly different from those obtained for inhibition of IL-1β release (Figure 7C-E), and similar to the ROS scavenger N-acetyl cystein (Figure 7E). Similarly, PPi and clodronate were able to block MTX-induced ROS production in M1 wildtype macrophages, but fails to block

P2X7R-induced ROS production from the same cells (Figure 7E), this could explain the underlying mechanism for the differential activation of the inflammasome by ATP and MTX observed between M1 and intermediate polarized macorphages (Figures 3A, 4F). Finally, MTX-stimulation of ROS production and its inhibition by ATP and PPi were not significantly altered by treatment with cytochalasin B (Figure 7F).

DISCUSSION

The concept of monocytes/macrophages existing in functionally distinct phenotypes from pro- to anti-inflammatory states has been well established by detailed studies on M1 (classically activated) and M2 (alternatively activated) macrophages (Gordon, 2003; Scotton et al., 2005; Martinez et al., 2006; 2008). But only recently has it begun to be appreciated that macrophages are able to reversibly and dynamically switch from one activation state to the other (Stout and Suttles, 2004; Porcheray et al., 2005; Gratchev et al., 2006). Here we have employed a polarization gradient of cytokines and endotoxin to rapidly generate a 5-stage *in vitro* model of macrophage polarization from M1 through M2. In states 1 – 4 intracellular IL-1β remained high and all stimuli except ATP continued to activate the inflammasome and release IL-1β. In intermediate polarization states, as well as in $P2X_7R$-deficient macrophages, ATP no longer signaled to caspase-1 activation; rather, ATP now acted via its diphosphate and/or triphosphate chains independently of any other purine receptor to block activation of the NLRP3 inflammasome by other activators. This was accomplished by two independent mechanisms: a direct reduction of ROS production and a rapid trapping of the inflammasome complex due to dramatic intracellular clustering of the actin cytoskeleton. Our results suggest this uncoupling of $P2X_7R$ from caspase-1 activation may prove to be a key trigger in the switch from a pro-inflammatory macrophage towards its alternative functions in the resolution of inflammation. Moreover, we have identified a new cellular mechanism by which the inflammasome can be inhibited via physiological alterations in the cytoskeleton.

The characteristics of $P2X_7R$-induced release of IL-1β from M1 activated macrophages are well established: intracellular pro-caspase-1 is rapidly cleaved and mature IL-1β, as well as caspase-1 and other inflammasome components (e.g. ASC) are released within minutes (2 – 10 min) after receptor stimulation (Mariathasan et al., 2004; 2006; Ferrari et al., 2006; Pelegrin and Surprenant, 2006). In the present study we compared these established properties of $P2X_7R$ activation in M1 macrophages with those of macrophages exposed to a gradient of M1 to M2 activation. We have focused on the intermediate polarization state (state 3) in wildtype mouse macrophages because it provides us with a representation of a macrophage on the cusp between M1 and M2 phenotypes. In state 3 intermediate polarized macrophages

intracellular levels of pro-IL-1β were similar to M1 macrophages, and $P2X_7R$ mRNA levels, protein levels and protein localization patterns showed no clear differences from M1 macrophages. Initial upstream signaling events which occur in the seconds to minute time scale and represent opening of the cation-permeable ion channel (calcium, sodium influx/potassium efflux) and the $P2X_7R$-pannexin-1 associated large pore (dye-uptake) (Pelegrin and Surprenant, 2006; 2007), were also the same as in M1 macrophages. *E. coli*, maitotoxin or nigericin-induced IL-1β release was the same as, or significantly increased, in these macrophages but ATP-induced release and caspase-1 activation were decreased by 50 – 80% due to an uncoupling of $P2X_7R$ signaling to ROS production and caspase-1 activation. Most strikingly, when ATP was co-applied with any of these other NLRP3 inflammasome activators, caspase-1 activation and IL-1β release were virtually abolished. Taken together, these results suggest that a specific uncoupling of $P2X_7R$ from the downstream caspase-1 cascade was occurring in intermediate state polarized macrophages without changes in receptor activation *per se* or its initial ion channel/dye-uptake pore activation.

We initially supposed that such an uncoupling of $P2X_7R$ from the inflammasome allowed ATP to now have a negative action on IL-1β release induced by other stimuli via one, or more, other purine receptor. But we found that ATP blocked *E.coli*, maitotoxin and nigericin-induced caspase-1 activation and IL-1β release in these macrophages by an action that did not involve other purine or adenosine receptors. This is a valid conclusion because agonist profiles did not correspond to any of these receptors, generic P2X and P2Y antagonists (suramin and PPADS) did not alter the inhibition by ATP observed in $P2X_7R$-deficient macrophages and, unequivocally, because pyrophosphates (tri and di, but not mono, phosphates) as well as the non-hydrolyzable bisphosphonate, clodronate, inhibited caspase-1 activation and IL-1β with potency order of clodronate > triphosphate ≈ diphosphate > ATP >> ADP, suggesting that the diphosphate group resident in ADP could partially block inflammasome without involvement of PPi metabolism. It is tempting to speculate that ecto-nucleotidases may play a critical role in the switch of a macrophage from an M1 to an M2 state during inflammatory resolution but future studies of expression levels and activities of the large family of these molecules (Zimmerman, 2000) are likely to provide insight into whether specific ecto-nucleotidases may play a critical role in the switch of a macrophage from an M1 to an

M2 state during inflammatory resolution. In any event, our results show that when $P2X_7Rs$ are fully functional, i.e. when they couple to inflammasome activation in M1 macrophages, the actions of ATP are solely stimulatory on IL-1β release. That is, neither PPi nor clodronate inhibited ATP-mediated IL-β release from M1 macrophages, nor even from state 3 intermediate polarized macrophages where the $P2X_7R$-specific IL-1β release was still present although at a much reduced level, while they effectively blocked maitotoxin and *E.coli*-induced inflammasome activation. These results further support our suggestion that a specific uncoupling of otherwise functional $P2X_7Rs$ from the caspase-1 cascade is the key event in the switch of ATP from inducing (via $P2X_7R$) to inhibiting (via PPP/PPi) IL-1β release (Figure 8). Recent pharmacological studies have shown that ROS production in M1 macrophages is a critical step for activation of the NLRP3 inflammasome in response to ATP, toxins or crystals (Dostert et al., 2008; Hewinson et al., 2008) and $P2X_7R$ activation recruits to the plasma membrane and activates NADPH oxidase complex (Hewinson et al., 2008). However, a recent study has not found genetic support for the role of ROS in NLRP3 inflammasome activation (Hornung et al., 2008). Here we found that in M2 macrophages $P2X_7R$ activation induces only a weak ROS response that may be due to a specific uncoupling from recruitment of the NADPH oxidase complex without alterations in $P2X_7R$ up-stream signaling, correlating with the low level of NLRP3-activation and IL-1β release found in intermediate polarized macrophages after ATP/$P2X_7R$ stimulation.

By imaging individual macrophages using a caspase-1-specific fluorescent probe and co-labelling for actin, or ASC as an integral component in the inflammasome complex, we found that $P2X_7R$ activation in M1 macrophages not only induced rapid actin cytoskeletal rearrangements along a spatial gradient but also rapid formation of active caspase-1/ASC aggregates which we interpret as likely sites of functionally active inflammasomes. Several of these aggregates tightly abutted the external surface of actin filaments outlining the plasma membrane, suggesting potential sites of release. In striking contrast, ATP applied to $P2X_7R$-depleted M1 macrophages, or to state 3 intermediate polarized macrophages, produced a rapid and intense intracellular clustering of actin filaments. A similar pattern of intracellular clustering of actin was observed when ATP, pyrophosphate or clodronate was co-applied with maitotoxin to these macrophages with little or no activated caspase-1

fluorescence signals. Cytochalasin B blocked this intracellular aggregation of actin and reversed by 30 - 50% the inhibition of release observed in the presence of maitotoxin plus ATP or pyrophosphate. Thus, we have identified intracellular clustering of actin filaments as a novel mechanism for inhibition of inflammasome activation (Figure 8).

The present study has direct and immediate clinical and physiological relevance. Clodronate and other bisphosphonates have been in clinical use for decades, primarily for the treatment of osteoarthritis and other inflammatory or metastatic bone diseases (Maksymowych, 2002; Russell et al., 2008). Their primary mechanism of action is generally considered to be one of effective chelation of calcium crystal deposits on bone mineral surfaces, resulting in inhibition of osteoclast apoptosis and bone resorption (Russell et al., 2008). On the other hand, several studies have provided evidence that they may also exert an anti-inflammatory action in bone and immune cells independent of their calcium chelation properties (Maksymowych, 2002; Pannanen et al., 1995). The pyrophosphate actions to inhibit IL-1β release identified in the present study may underlie these anti-inflammatory actions of bisphosphonates. A novel, highly selective and potent $P2X_7R$ antagonist, AZ9056, is currently in clinical trials for rheumatoid arthritis (McInnes et al., 2007). Studies to date point to the primary mechanism of action of such $P2X_7R$ antagonists as being via inhibition of IL-1β release (Labasi et al., 2002; Pelegrin, 2008). Our present work continues to support this conclusion but now raises the possibility that a secondary effect of $P2X_7R$ inhibition is to further inhibit IL-1β release evoked by other activators by allowing pyrophosphates – either via extracellular ATP metabolism or directly via the phosphate chains of the intact nucleotides - to directly prevent inflammasome activation by other bacterial or endogenous inflammatory pathogen associated molecular patterns via inhibition of ROS production and by intracellular trapping of the inflammasome complex. Clinical investigations into the potential of co-therapy with $P2X_7R$ antagonists and bisphosphonates in chronic inflammatory diseases may prove fruitful.

MATERIALS AND METHODS

Cells and Reagents

Key reagents and their sources: *E. coli* LPS O55:B5, ATP, ADP, AMP, adenosine, PPi, triphosphates, N-acetyl cystein, α-tocopherol, nigericin (Sigma); maitotoxin (Alexis); clodronate, Caspase-1 Substrate (N^a-5-Tetramethylrhodaminyl-YVADAC(S-acrylodan)-OH), cytochalasin B (Calbiochem); IFNγ, IL-4 and IL-1β (PeproTech). *E. coli* DH5α strain, DAPI, phalloidin-Texas Red and OxyBURST® H_2HFF-BSA (Invitrogen). Abs for ELISAs and cathepsin L were from R&D, for $P2X_7R$ from Alamone Laboratories, caspase-1 p10 rabbit polyclonal and β-actin from Santa Cruz Biotechnology, ASC from Alexis, IL-1β mAb from the Biological Resources Branch, National Cancer Institute. All HRP-conjugated secondary Abs were from DAKO Cytomation. A740003 $P2X_7R$ antagonist was synthesized by ArtMolecule.

C57BL/6J ($P2X_7R^{+/+}$) and $P2X_7R$-deficient ($P2X_7R^{-/-}$) mice in C57BL/6J background were used (Chessell et al., 2005). All experiments were carried out under the Animals (Scientific Procedures) Act 1986. Peritoneal macrophages were obtained as previously described (Pelegrin and Surprenant, 2006). Briefly, the peritoneal cavity was gently lavaged with phosphate-buffered saline (PBS, Invitrogen). The recovered buffer from two to three mice was pooled, cells were collected by centrifugation (250 x g, 5 min) and plated on coverslips, or in 12-well plates at a density of 10^6 cell/well, or in 24-well plates at a density of 0.5 x 10^6 cell/well, or in 96-well plates black with clear bottom at a density of 1.5 x 10^6 cell/well in RPMI 1640 media (Invitrogen) supplemented with 10% fetal calf serum (Invitrogen), 100 units/ml penicillin and 100 μg/ml streptomycin (Invitrogen). The macrophages were allowed to adhere overnight (37°C, 5% CO_2) and washed with fresh medium to remove unattached cells before use.

Cell culture and stimulation

Macrophages plated on 12-well plates were primed with fresh medium supplemented with different stimuli to obtain a gradient of polarity phenotypes (Figure S1A). For clarity, the different polarity phenotypes have been represented in the figures and in the text with a number, a color and a shape. LPS (1 μg/ml) and IFNγ (20 ng/ml) for 4 h were used to differentiate to M1 phenotype (polarity state 1, square, red). IL-4 (20 ng/ml) was used for 4 h to differentiate to M2 phenotype (polarity state 5, round,

blue). A combination of LPS/IFNγ/IL-4 for 4 h was used to differentiate a M1/M2 intermediate macrophage polarization phenotype (polarity state 3, diamond, green). To study the polarity changes and to achieve intermediate polarity states, cells were stimulated first for 4 h with IL-4, washed and then stimulated for further 4 h with LPS/IFNγ (polarity state 2, star, pink); or stimulated first for 4 h with LPS/IFNγ, washed and then stimulated for further 4 h with IL-4 (polarity state 4, triangle, yellow). Macrophages were stimulated for 15 min with agonists as described previously (Pelegrin and Surprenant, 2007). Alternatively, to examine the blocking of IL-1β release, macrophages were incubated with 0.01 – 5 mM of ATP, PPi, triphosphate or clodronate or with 5 mM of ADP, AMP, AD or Pi or with 20 mM N-acetyl cystein or 10 μM α-tocopherol together with MTX (0.2 nM). *E. coli* stimulation was carried out as described previously (Petrilli et al., 2007). Macrophages were stimulated either with LPS/IFNγ (polarity state 1), IL-4 (polarity state 5) or with a combination of LPS/IFNγ/IL-4 (polarity state 3) for 2 h, washed in Optimem and challenged with *E. coli* for 1 h in the presence or absence of ATP (0.1 - 5 mM); the cells were then washed and placed in Optimem complemented with 100 units/ml penicillin and 100 μg/ml streptomycin for further 4 hours.

Western blot, ELISAs, intracellular calcium and dye uptake assays

Detailed methods used for Western blot analysis, ELISAs, Fura2 calcium imaging and ethidium bromide uptake have been described previously (Pelegrin and Surprenant, 2006). Blots were analyzed by densitometry measurements using NIH ImageJ software (http:// rsb.info.nih.gov/ij/).

Immunocytochemistry and microscopy

Macrophages stimulated on coverslips were washed twice with PBS, fixed with 4% formaldehyde for 30 min at room temperature, and then washed three times with PBS. Cells were blocked with 3 % bovine serum albumin and permeabilized with 0.1 % triton X-100 in PBS for 30 min at room temperature before incubating with rat anti-mouse F4/80 antibody (1:500), rabbit anti-$P2X_7R$ (1:500), rabbit anti-ASC (1:250) or with goat anti-cathepsin L (1:250) for 18–20 h at 4°C or for 2 h at room temperature. Cells were washed and incubated with appropriate FITC-, TRITC- or Cy3-conjugated secondary antibody (1:200) for 2 h at room temperature, then rinsed in PBS and

incubated for 15 min with 300 nM of DAPI and in some experiments with phalloidin-Texas Red (1:100). To stain for active caspase-1, macrophages were activated with 5 mM ATP or 0.2 nM MTX for 5 min at 37ºC, washed and incubated with the fluorochrome inhibitor of caspase-1, green fluorescent peptide 5-carboxyfluorescein-Tyr-Val-Ala-Asp-fluoromethyl ketone (FAM-YVAD-fmk), according to the manufacturer's recommendations (Immunochemistry Technologies). Cells were fixed with 4% formaldehyde, blocked, permeabilized and co-stained for F-actin (phalloidin-Texas Red), ASC or cathepsin L. All coverslips were mounted on slides with ProLong Gold Antifade Reagent (Invitrogen). Images were acquired at room temperature on a Delta Vision RT (Applied Precision) restoration microscope using a 60x/1.42 Plan Apo or 100x/1.40 Uplan Apo objectives and the 360nm/475nm, 490nm/528nm and 555nm/617nm filter sets (Chroma 86000v2). The images were collected using a Coolsnap HQ (Photometrics) camera with a Z optical spacing of 0.2 μm. Raw images were then deconvolved using Softworx software and maximum intensity projections of these deconvolved images are shown in the results. ImageJ software (http:// rsb.info.nih.gov/ij/) was used to quantify images.

Quantitative Reverse Transcriptase-PCR Analysis

Detailed methods used for qRT-PCR have been described previously (Pelegrin and Surprenant, 2006). Specific primers were purchased from Qiagen (QuantiTech Primer Assays), for each primer set the efficiency was > 95% and a single product was seen on melt curve analysis. Relative expression levels were calculated using the $2^{-\Delta\Delta Ct}$ method normalizing to GAPDH expression levels for each treatment and the fold increase in expression was relative to the smallest expression level.

Caspase-1 activity and reactive oxygen species measurement

Macrophages were plated in a 96-well plate black with clear bottom and primed to reach different polarity states. For casapse-1 activity cells were pre-incubated with 37.5 μM TMR-YVADAC(AD) at 37 ºC for 1 h and washed twice with E-total. Fluorescence was recorded using FlexStation 3 over 30 min at 1 min intervals at 380 nm for excitation and 525 nm for the emission. ATP (5 mM) was added into the wells automatically by the machine at designated time points. For reactive oxygen species (ROS) generation, polarized macrophages were washed with PBS and

incubated with ATP, clodronate, PPi (0.1 - 5 mM) or N-acetyl cystein (20 mM) and/or MTX (0.2 nM) in the presence of 10 μg/ml H_2HFF-BSA and fluorescence emmision by the oxidation of H_2HFF-BSA was recorded by FlexStation 3 over 60 min at 1 min intervals at 492 nm for excitation and 520 nm for the emission.

Statistical analysis

Average results are expressed as the mean ± s.e.m. from the number of assays indicated (from at least three separate cultures). Data were analyzed by an unpaired two-tailed Student's t-test to determine difference between groups using Prism and Instat (GraphPad) software.

ACKNOWLEDGMENTS

We thank Elizabeth Martin, Austen Sitko and Mari-Carmen Banos-Gregori for technical support. This work was supported by the Wellcome Trust.

ABBREVIATIONS

A740003: *N*-1-{[(cyanoimino) (5-quinolinylamino) methyl] amino}-2,2-dimethylpropyl)-2-(3,4-dimethoxyphenyl) acetamide; AD: Adenosine; ASC: Apoptosis-associated Speck-like protein containing a C-terminal Caspase-activating recruiting domain; CB: Cytochalasin B; E-NPP: Ectonucleotide pyrophosphatase; E-NTPDase1: Ecto-nucleoside triphosphate diphosphohydrolase-1; GAPDH: Glyceraldehyde 3-phosphate dehydrogenase; IL: Interleukin; LPS: Lipopolysaccharide; M1: classical activated macrophages; M2: alternative activated macrophages; MRC-1: Mannose Receptor C-1; MTX: maitotoxin; NAC: N-acetyl cystein; NLRP3: Nucleotide-binding domain and Leucine-rich repeat Receptor containing Pyrin domain 3; $P2X_7R$: $P2X_7$ receptor; PAMP: Pathogen-Associated Molecular Pattern; PPi: Pyrophosphate; PPP: Triphosphates; ROS: Reactive Oxygen Species.

SUPPLEMENTARY INFORMATION IS AVAILABLE AT THE EMBO JOURNAL ONLINE

REFERENCES

Arend WP, Gordon DF, Wood DM, Janson RW, Joslin FG, Jameel S (1989) IL-1 beta production in cultured human monocytes is regulated at multiple levels. *J Immunol* **143**: 118-126

Brough D, Rothwell N (2007) Caspase-1-dependent processing of pro-interleukin-1beta is cytosolic and precedes cell death. *J Cell Sci* **120**: 772-781

Chessell IP, Hatcher JP, Bountra C, Michel AD, Hughes JP, Green P, Egerton J, Murfin M, Richardson J, Peck WL, Grahames CB, Casula MA, Yiangou Y, Birch R, Anand P, Buell GN (2005) Disruption of the P2X7 purinoceptor gene abolishes chronic inflammatory and neuropathic pain. *Pain* **114**: 386-396

Dinarello CA (1996) Biologic basis for interleukin-1 in disease. *Blood* **87**: 2095-2147

Dombrecht EJ, De Tollenaere CB, Aerts K, Cos P, Schuerwegh AJ, Bridts CH, Van Offel JF, Ebo DG, Stevens WJ, De Clerck LS (2006) Antioxidant effect of bisphosphonates and simvastatin on chondrocyte lipid peroxidation. *Biochem Biophys Res Commun* **348**: 459-464

Dostert C, Pétrilli V, Van Bruggen R, Steele C, Mossman BT, Tschopp J (2008) Innate immune activation through Nalp3 inflammasome sensing of asbestos and silica. *Science* **320**: 674-677

Ehrt S, Schnappinger D, Bekiranov S, Drenkow J, Shi S, Gingeras TR, Gaasterland T, Schoolnik G, Nathan C (2001) Reprogramming of the macrophage transcriptome in response to interferon-gamma and *Mycobacterium tuberculosis*: signaling roles of nitric oxide synthase-2 and phagocyte oxidase. *J Exp Med* **194**: 1123-1140

Ferrari D, Pizzirani C, Adinolfi E, Lemoli RM, Curti A, Idzko M, Panther E, Di Virgilio F (2006) The P2X7 receptor: a key player in IL-1 processing and release. *J Immunol* **176**: 3877-3883

Gordon S (2003) Alternative activation of macrophages. *Nat Rev Immunol* **3**: 23-35

Gratchev A, Kzhyshkowska J, Köthe K, Muller-Molinet I, Kannookadan S, Utikal J, Goerdt S (2006) Mphi1 and Mphi2 can be re-polarized by Th2 or Th1 cytokines, respectively, and respond to exogenous danger signals. *Immunobiology* **211**: 473-486

Hewinson J, Moore SF, Glover C, Watts AG, MacKenzie AB (2008) A key role for redox signaling in rapid P2X7 receptor-induced IL-1 beta processing in human monocytes. *J Immunol* **180**: 8410-8420

Honore P, Donnelly-Roberts D, Namovic MT, Hsieh G, Zhu CZ, Mikusa JP, Hernandez G, Zhong C, Gauvin DM, Chandran P, Harris R, Medrano AP, Carroll W, Marsh K, Sullivan JP, Faltynek CR, Jarvis MF (2006) A-740003 [N-(1-{[(cyanoimino) (5-quinolinylamino) methyl] amino} -2,2- dimethylpropyl) -2-(3,4-dimethoxyphenyl) acetamide], a novel and selective P2X7 receptor antagonist, dose-dependently reduces neuropathic pain in the rat. *J Pharmacol Exp Ther* **319**: 1376-1385

Hornung V, Bauernfeind F, Halle A, Samstad E, Kono H, Rock K, Fitzgerald KA, Latz E (2008) Silica crystals and aluminum salts activate the NALP3 inflammasome through phagosomal destabilization. *Nat Immunol* **9**: 847-856

Kachur AV, Manevich Y, Biaglow JE (1997) Effect of purine nucleoside phosphates on OH-radical generation by reaction of Fe2+ with oxygen. *Free Radic Res* **26**: 399-408

Kanneganti TD, Ozören N, Body-Malapel M, Amer A, Park JH, Franchi L, Whitfield J, Barchet W, Colonna M, Vandenabeele P, Bertin J, Coyle A, Grant E, Akira S, Nunez G (2006) Bacterial RNA and small antiviral compounds activate caspase-1 through cryopyrin/Nalp3. *Nature* **440**: 233-236

Labasi JM, Petrushova N, Donovan C, McCurdy S, Lira P, Payette MM, Brissette W, Wicks JR, Audoly L, Gabel CA (2002) Absence of the P2X7 receptor alters leukocyte function and attenuates an inflammatory response. *J Immunol* **168**: 6436-6445

Maksymowych WP (2002) Bisphosphonates - Anti-Inflammatory Properties. *Curr Med Chem* **1**: 15-28

Mariathasan S, Newton K, Monack DM, Vucic D, French D, Lee WP, Roose-Girma M, Erickson S, Dixit VM (2004) Differential activation of the inflammasome by caspase-1 adaptors ASC and Ipaf. *Nature* **430**: 213-218

Mariathasan S, Weiss DS, Newton K, McBride J, O'Rourke K, Roose-Girma M, Lee WP, Weinrauch Y, Monack DM, Dixit VM (2006) Cryopyrin activates the inflammasome in response to toxins and ATP. *Nature* **440**: 228-232

Martinez FO, Gordon S, Locati M, Mantovani A (2006) Transcriptional profiling of the human monocyte-to-macrophage differentiation and polarization: new molecules and patterns of gene expression. *J Immunol* **177**: 7303-7311

Martinez FO, Sica A, Mantovani A, Locati M (2008) Macrophage activation and polarization. *Front Biosci* **13**: 453-461

Martinon F, Burns K, Tschopp J (2002) The inflammasome: a molecular platform triggering activation of inflammatory caspases and processing of proIL-beta. *Mol Cell* **10**: 417-426

Martinon F, Pétrilli V, Mayor A, Tardivel A, Tschopp J (2006) Gout-associated uric acid crystals activate the NALP3 inflammasome. *Nature* **440**: 237-241

McInnes IB, Snell NJ, Perrett JH, Parmar H, Wang MM, Astbury C (2007) Results of a Phase II clinical trial of a novel P2X7 receptor antagonist, AZD9056, in patients with active rheumatoid arthritis (CREATE study). *ACR/ARHP Annual Scientific Meeting* presentation 2085

Pannanen N, Lapinjoki S, Urtti A, Monkkonen J (1995) Effect of liposomal and free bisphosphonates on the IL-1β, IL-6 and TNFα secretion from RAW 264 cells in vitro. *Pharm Res* **12:** 916-922

Pelegrin P, Surprenant A (2006) Pannexin-1 mediates large pore formation and interleukin-1beta release by the ATP-gated P2X7 receptor. *EMBO J* **25**: 5071-5082

Pelegrin P, Surprenant A (2007) Pannexin-1 couples to maitotoxin- and nigericin-induced interleukin-1beta release through a dye uptake-independent pathway. *J Biol Chem* **282**: 2386-2394

Pelegrin P (2008) Targeting interleukin-1 signaling in chronic inflammation: focus on P2X(7) receptor and Pannexin-1. *Drug News Perspect* **21**: 424-433

Pelegrin P, Barroso-Gutierrez C, Surprenant A (2008) P2X7 receptor differentially couples to distinct release pathways for IL-1beta in mouse macrophage. *J Immunol* **180**: 7147-7157

Pétrilli V, Papin S, Dostert C, Mayor A, Martinon F, Tschopp J (2007) Activation of the NALP3 inflammasome is triggered by low intracellular potassium concentration. *Cell Death Differ* **14**: 1583-1589

Pfeiffer ZA, Aga M, Prabhu U, Watters JJ, Hall DJ, Bertics PJ (2004) The nucleotide receptor P2X7 mediates actin reorganization and membrane blebbing in RAW 264.7 macrophages via p38 MAP kinase and Rho. *J Leukoc Biol* **75**: 1173-1182

Porcheray F, Viaud S, Rimaniol AC, Léone C, Samah B, Dereuddre-Bosquet N, Dormont D, Gras G (2005) Macrophage activation switching: an asset for the resolution of inflammation. *Clin Exp Immunol* **142**: 481-489

Romagnani S (2000) T-cell subsets (Th1 versus Th2). *Ann Allerg Asthma Im* **85**: 9-18

Russell RG, Watts NB, Ebetino FH, Rogers MJ (2008) Mechanisms of action of bisphosphonates: similarities and differences and their potential influence on clinical efficacy. *Osteoporos Int* **19**: 733-759

Scotton CJ, Martinez FO, Smelt MJ, Sironi M, Locati M, Mantovani A, Sozzani S (2005) Transcriptional profiling reveals complex regulation of the monocyte IL-1 beta system by IL-13. *J Immunol* **174**: 834-845

Serretti R, Core P, Muti S, Salaffi F (1993) Influence of dichloromethylene diphosphonate on reactive oxygen species production by human neutrophils. *Rheumatol Int* **13**: 135-138

Stout RD, Suttles J (2004) Functional plasticity of macrophages: reversible adaptation to changing microenvironments. *J Leukocyte Biol* **76**: 509-513

van Rooijen N, Sanders A (1994) Liposome mediated depletion of macrophages: mechanism of actions, preparation of liposomes and application. *J Immunol Methods* **174:** 83-93

van Rooijen N, Sanders A (1997) Elimination, blocking and activation of macrophages: three of a kind? *J Leukocyte Biol* **62:** 702-709

Verhoef PA, Kertesy SB, Estacion M, Schilling WP, Dubyak GR (2004) Maitotoxin induces biphasic interleukin-1beta secretion and membrane blebbing in murine macrophages. *Mol Pharmacol* **66**: 909-920

Zimmermann H (2000) Extracellular metabolism of ATP and other nucleotides. *Naunyn Schmiedebergs Arch Pharmacol* **362**: 299-309

Figure Legends

Figure 1. **Functional macrophage plasticity during a polarization gradient.** (A and B) Deconvolved images of peritoneal macrophages during polarization gradient (conditions from 1 to 5, see methods) immunostained for mouse macrophage surface marker F4/80 (A) or labeled with Texas Red-phalloidin to reveal F-actin cytoskeleton (B). Images are representative of three independent experiments; bar = 5 μm. (C) Cellular area measure from peritoneal macrophage during polarization gradient; *n* = 50 to 70 cells from three independent experiments. Horizontal bars represent medians, boxes represent the 25th and 75th percentiles, and vertical bars represent ranges; ** $p < 0.001$. (D) Real-time quantitative RT-PCR for classical M1 (TNFα) and M2 (mannose receptor C type 1, MRC-1) genes and $P2X_7R$ gene during macrophage polarization gradient. Data is average of triplicate reactions and representative of 3 independent experiments.

Figure 2. **$P2X_7R$ signaling during macrophage polarization gradient.** (A) IL-1β or β-actin immunoblot of murine peritoneal macrophage lysates and supernatants during a polarization gradient from M1 towards M2 (conditions from 1 - 5, see methods) in the presence or absence of 5 mM ATP (15 min). ATP does not release IL-1β in states 3 and 4 despite high levels of intracellular pro-IL-1β; blots are representative of 3 independent experiments. (B and C) ELISA comparing intracellular production and release of IL-1β by mouse peritoneal macrophages induced by ATP (5 mM for 15 min) or *E. coli* (4 h) after 4 h of polarization to M1 (1, red: LPS and IFNγ), to M2 (5, blue: IL-4) or to intermediate polarization state (3, green: LPS, IFNγ and IL-4) (B) or after priming for 0 to 24 h with LPS and IFNγ (C); *n* = 3 independent cultures for each condition, *p = 0.0483, **p=0.0014. (D) Deconvolved images of M1 (left panel) or M2 (right panel) polarized peritoneal macrophages immunostained for F4/80 (red) and for $P2X_7R$ (green). Bar, 5 μm. (E) Fura2 fluorescence ratio recorded from peritoneal macrophages isolated from $P2X_7R^{+/+}$ or $P2X_7R^{-/-}$ mice polarized to M1, M2 or to an intermediate polarization state. $P2X_7R$ receptors were activated with ATP (1 mM) resulting in typical sustained intracellular calcium increase. Traces are the average of 4 – 6 independent cultures and representative of 3 independent experiments. (F) Kinetics of dye uptake (ethidium bromide fluorescence) in peritoneal macrophages isolated from $P2X_7R^{+/+}$ or

$P2X_7R^{-/-}$ mice polarized to M1, M2 or to an intermediate polarization state in response to 5 mM ATP, *n* = 3 independent experiments in each case.

Figure 3. **Switch from positive to negative regulation of IL-1β release by ATP during macrophage polarization gradient.** (A) IL-1β release by M1 polarized (1: LPS and IFNγ) or intermediate polarized (3: LPS, IFNγ and IL-4) mouse peritoneal macrophages activated for 15 min with ATP (5 mM), maitotoxin (MTX, 0.2 nM) or a combination of ATP and MTX detected by ELISA; *n* = 3 independent cultures for ELISA; *p=0.0121; **p=0.0013. (B) IL-1β release by M1 polarized mouse peritoneal macrophages induced by 15 min of ATP (5 mM), MTX (0.2 nM) or a combination of ATP and MTX in the presence of absence of $P2X_7R$ antagonist A740003 (10 μM, 5 min before ATP/MTX) detected by by immunoblot; blots are representative of 3 independent experiments. (C) Immunoblots for intracellular IL-1β (top panels), released IL-1β (middle panels) and released active caspase-1 (p10 subunit, bottom panels) in M1 polarized peritoneal macrophages from $P2X_7R^{+/+}$ or $P2X_7R^{-/-}$ mice stimulated for 15 min with ATP (5 mM), maitotoxin (MTX, 0.2 nM), nigericin (5 μM) or a combination of ATP and MTX or ATP and nigericin; blots are representative of 3 to 13 independent experiments. (D) Immunoblots for intracellular (top panel) and released (bottom panel) ASC in M1 polarized peritoneal macrophages from $P2X_7R^{-/-}$ mice stimulated during 15 min with ATP (5 mM), MTX (0.2 nM) or a combination of ATP and MTX; blots are representative of 2 independent experiments. (E) Representative traces for caspase-1 activity in M1 or M2 polarized peritoneal macrophages from $P2X_7R^{+/+}$ or $P2X_7R^{-/-}$ mice monitored over 30 min with the fluorescent probe TMR-YVADAC(AD) after stimulation with 5 mM ATP. Traces are the average of 4 independent cultures and are representative of 2 independent experiments. (F) $P2X_7R^{-/-}$ M1 polarized peritoneal macrophages were challenged with *E. coli* for 1 h in the absence or presence of 5 mM ATP and further incubated for 4 h, IL-1β was detected by immunoblot. Blots are representative of 3 independent experiments.

Figure 4. **Negative regulation of IL-1β release by ATP is not due to a purine receptor but to pyrophosphate action.** (A-C) Inhibition of MTX (0.2 nM, 15 min) induced IL-1β release in M1 polarized peritoneal macrophages from $P2X_7R^{-/-}$ with the

indicated concentrations of ATP (A) or 5 mM of ATP, ADP, AMP, adenosine (AD) or 0.1 or 5 mM of pyrophosphate (PPi) (B,C); Immunoblots for intracellular IL-1β (top panels), released IL-1β (middle panels) or released active caspase-1 (p10 subunit, bottom panels) (A,B) or ELISA for released IL-1β (C). (D) Immunoblots for intracellular IL-1β (top panel) or released IL-1β (bottom panel) in M1 polarized peritoneal macrophages from $P2X_7R^{-/-}$ mice stimulated for 15 min with MTX (0.2 nM) and 5 mM of ATP, PPi, inorganic phosphate (Pi) or 1 mM clodronate. (E) Concentration-inhibition curves (solid symbols) of IL-1β release in M1 polarized peritoneal macrophages from $P2X_7R^{-/-}$ mice stimulated with MTX (0.2 nM, 15 min) in the presence or absence of different concentrations of ATP (triangles), PPi (circles) or clodronate (squares). Concentration-response curve (open diamonds) of IL-1β release in M1 polarized peritoneal macrophages from $P2X_7R^{+/+}$ mice stimulated with different concentrations of ATP (15 min); n = 3 for each point. (F) Immunoblots for released IL-1β of M1 polarized (1: LPS and IFNγ) or intermediate polarized (3: LPS, IFNγ and IL-4) polarized peritoneal macrophages from $P2X_7R^{+/+}$ mice stimulated for 15 min with MTX (0.2 nM) or ATP (5 mM) in the presence or absence of PPi (5 mM), clodronate (1 mM) or Pi (5 mM). *n* = 3 independent cultures for ELISA and blots are representative of 2 to 3 independent experiments.

Figure 5. **ATP differentially regulates actin polymerization during macrophage polarity gradient.** (A) Deconvolved images of F-actin cytoskeleton labeled with Texas Red-phalloidin in peritoneal macrophages isolated from $P2X_7R^{+/+}$ or $P2X_7R^{-/-}$ mice after differentiation to M1 or to intermediate state 3 polarization state, unstimulated or stimulated for 5 min with ATP (5 mM), MTX (0.2 nM) or a combination of ATP and MTX, in the presence or absence of A740003 (10 μM, 5 min before ATP). Bar, 5 μm. Images are representative of three independent experiments. (B and C) M1 polarized peritoneal macrophages isolated from $P2X_7R^{-/-}$ mice were treated with cytochalasin B (CB; 2.5 μg/ml, 5 min before MTX) and stimulated for 15 min with MTX (0.2 nM) or a combination of MTX and ATP (5 mM) or PPi (3 mM), and IL-1β release was detected by immunoblots (B) or by ELISA (C); *n* = 3 independent cultures for ELISA and representative of 2 independent experiments, blots are representative of 2 independent experiments.

Figure 6. **Cellular dynamics and localization of the inflammasome.** (A) Deconvolved images of $P2X_7R^{+/+}$ M1 polarized peritoneal macrophages stained for active caspase-1 (green) and F-actin cytoskeleton (red, left panels), ASC (red, middle panels) or cathepsin L (red, right panels), before (top panels) or after (bottom panels) stimulation with ATP (5 mM, 5 min). Arrows show active caspase-1 crossing actin barrier and presumably being released; co-localization of active caspase-1 with ASC (arrowheads) indicating active inflammasomes; note no colocalization between active casapse-1 and lysosomal marker cathepsin L. (B) M1 polarized peritoneal macrophages isolated from $P2X_7R^{-/-}$ mice labeled for active caspase-1 (green) and F-actin cytoskeleton with Texas Red-phalloidin (red) stimulated for 5 min with MTX (0.2 nM) alone or in combination with ATP (5 mM). Bar, 5 μm. Images are representative of two independent experiments.

Figure 7. **ATP modulation of ROS production during macrophage polarization.** (A-C) ROS production was monitored over 20 min with the fluorescent probe H_2HFF-BSA in M1 (A,C) or M2 (B) macrophages from $P2X_7R^{+/+}$ (A,B) or $P2X_7R^{-/-}$ (C) mice stimulated with ATP (5 mM), MTX (0.2 nM) or a combination of ATP and MTX; traces are the average of 3-4 independent cultures and are representative of 3 independent experiments. (D) Concentration-inhibition curves of ROS production induced by MTX (0.2 nM, 20 min) in the presence or absence of different concentrations of ATP (squares), PPi (circles) or clodronate (triangles) in $P2X_7R^{-/-}$ M1 macrophages; n = 3 for each point. (E) Average of 3 different experiments for ROS production at 20 min by M1 or M2 polarized macrophages from $P2X_7R^{+/+}$ (open bars) or $P2X_7R^{-/-}$ (grey bars) mice stimulated as in A-C, in the presence or absence of PPi (5 mM), clodronate (1 mM) or N-acetyl cystein (NAC, 20 mM); *p=0.0005; **p=0.0003; ***p=0.0002. (F) $P2X_7R^{-/-}$ M1 macrophages were treated with cytochalasin B (CB; 2.5 μg/ml, 5 min before MTX) and ROS production was induced by 20 min incubation at 37ºC with 0.2 nM of MTX in the absence or presence of 5 mM of ATP or 3 mM of PPi; n = 4 independent cultures and representative of 2 independent experiments.

Figure 8. **Proposed model for inflammasome regulation by extracelluar ATP during macrophage polarization gradient**. In M1 polarized macrophages ATP

acting through $P2X_7R$ is linked with an increase production of ROS, actin polymerization to the edge of the cell, activation of the NLRP3-inflammasome/caspase-1 and rapid release of the pro-inflammatory mature IL-1β cytokine. However, during the resolving phase of the inflammation M1 macrophages switch their phenotype towards M2 and now $P2X_7R$ uncouples to both ROS production and the NLRP3-inflammasome/caspase-1 pathway although it remains functional in terms of its ion channel activity. Under these conditions (intermediate state 3) the PPi group of ATP acts to further inhibit ROS and induces an intracellular clustering of actin that blocks the inflammasome/activation of caspase-1 and the release of mature IL-1β to enhance the resolving phase of the inflammation. The PPi may result from ATP metabolism by ecto-nucleotidases or may act by phosphate chains remaining attached to the nucleotide molecule.

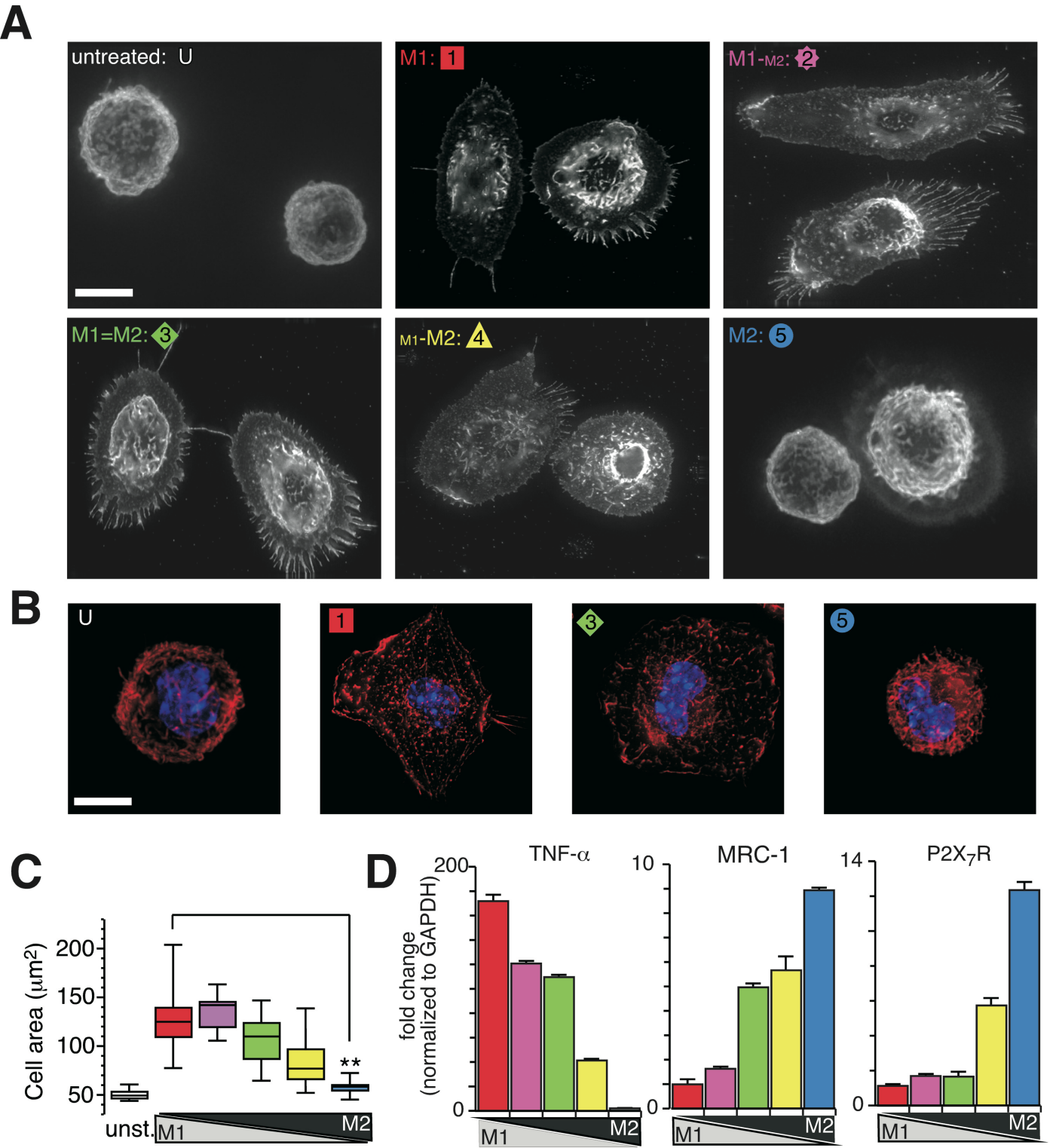
A
untreated: U
M1: 1
M1-M2: 2
M1=M2: 3
M1-M2: 4
M2: 5
B
U
1
3
5
C
Cell area (μm²)
200
150
100
50
unst.
M1
M2
**
D
TNF-α
MRC-1
P2X7R
fold change (normalized to GAPDH)
200
10
14
0
0
0
M1
M2
M1
M2
M1
M2

Figure 2

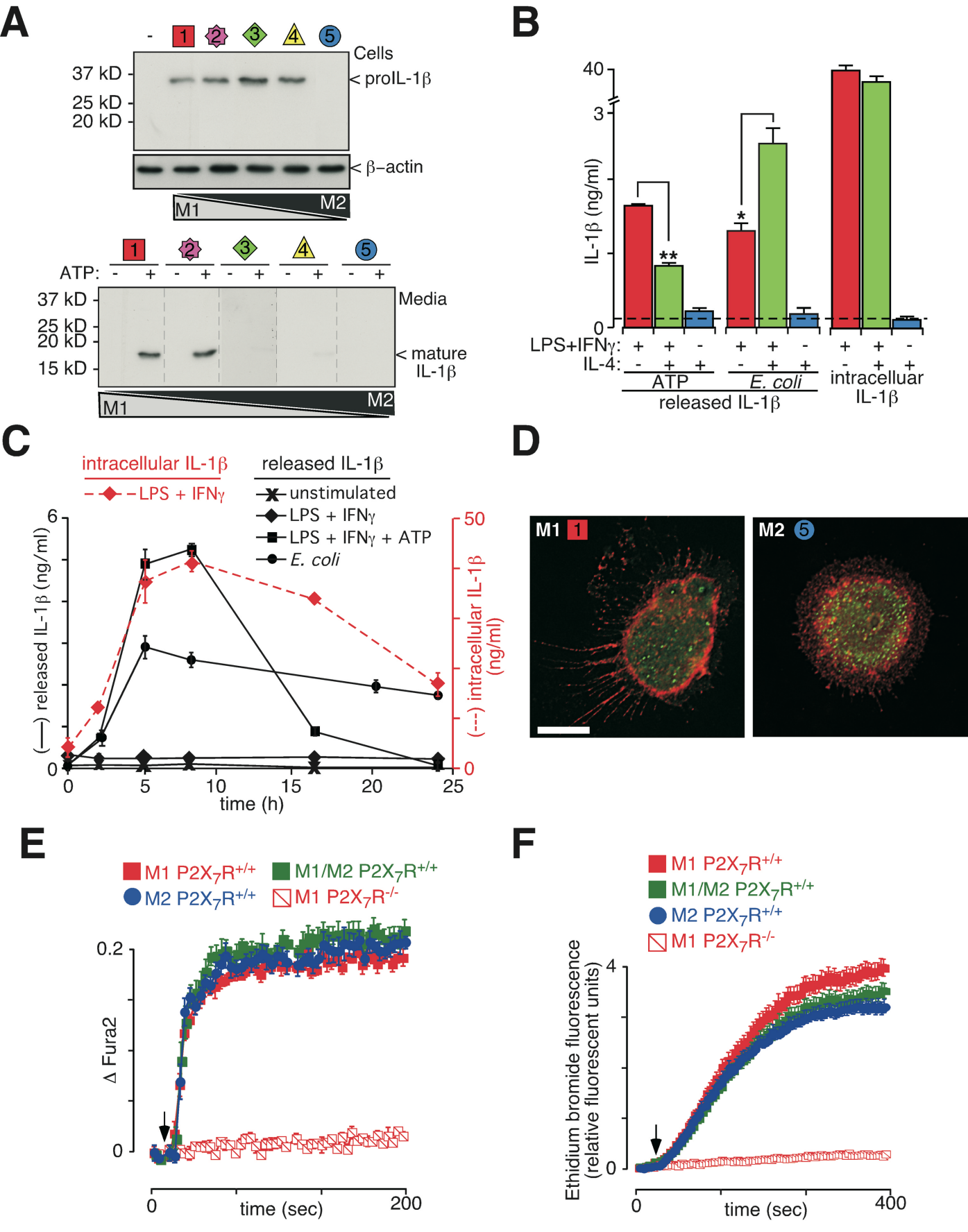
A
Cells
37 kD
25 kD
20 kD
< proIL-1β
< β–actin
M1
M2
ATP:
Media
15 kD
< mature IL-1β
B
IL-1β (ng/ml)
LPS+IFNγ:
IL-4:
ATP
E. coli
released IL-1β
intracellular IL-1β
C
intracellular IL-1β
LPS + IFNγ
released IL-1β
unstimulated
LPS + IFNγ + ATP
E. coli
(—) released IL-1β (ng/ml)
(---) intracellular IL-1β (ng/ml)
time (h)
D
M1
M2
E
M1 P2X7R+/+
M1/M2 P2X7R+/+
M2 P2X7R+/+
M1 P2X7R-/-
Δ Fura2
time (sec)
F
Ethidium bromide fluorescence (relative fluorescent units)
time (sec)

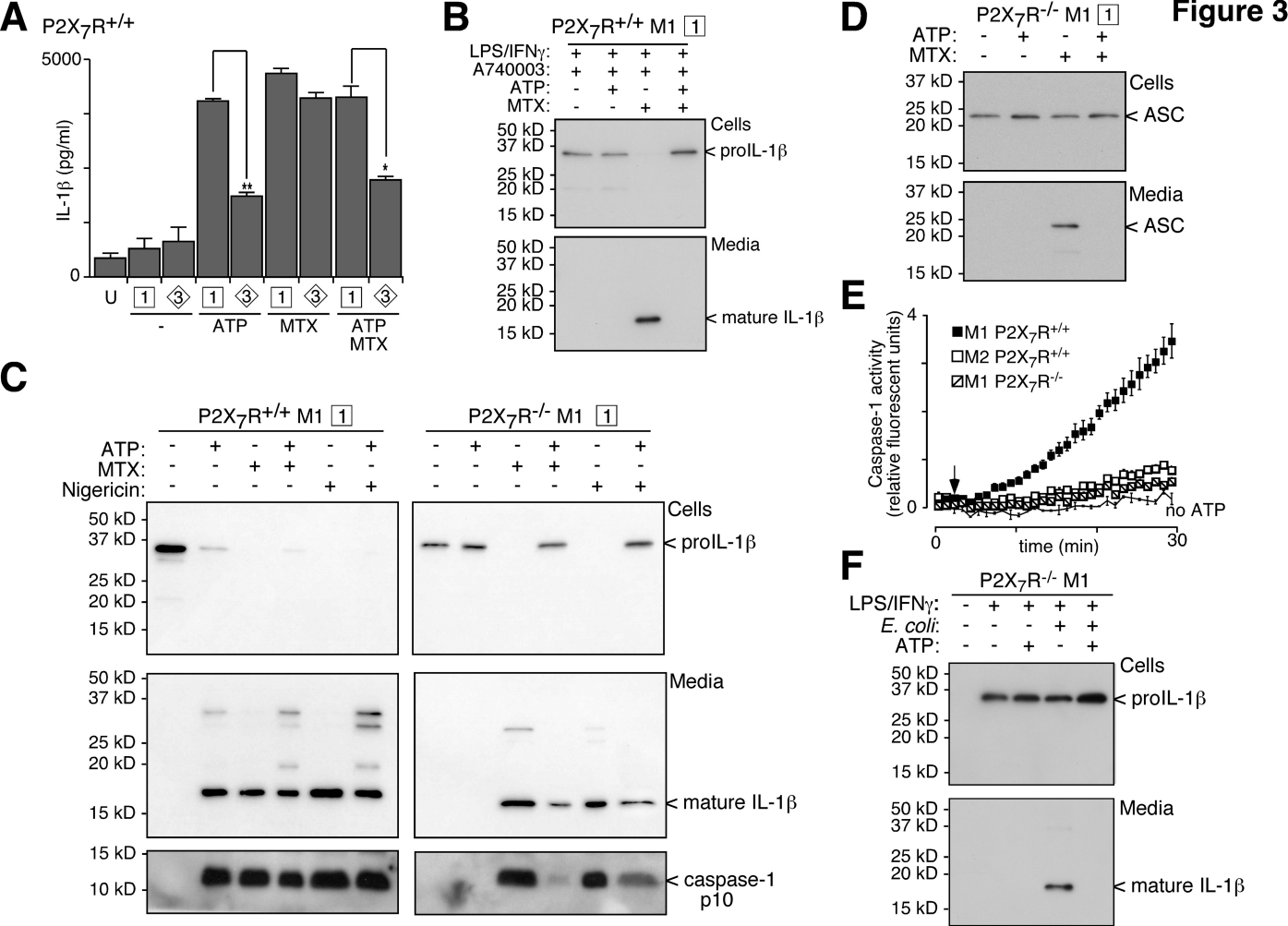
A
P2X7R+/+
5000
IL-1β (pg/ml)
0
U
1
3
-
ATP
MTX
ATP MTX
B
P2X7R+/+ M1 1
LPS/IFNγ:
A740003:
ATP:
MTX:
50 kD
37 kD
25 kD
20 kD
15 kD
Cells
proIL-1β
Media
mature IL-1β
C
P2X7R+/+ M1 1
P2X7R-/- M1 1
ATP:
MTX:
Nigericin:
Cells
proIL-1β
Media
mature IL-1β
15 kD
10 kD
caspase-1 p10
D
P2X7R-/- M1 1
ATP:
MTX:
Cells
ASC
Media
ASC
E
Caspase-1 activity (relative fluorescent units)
M1 P2X7R+/+
M2 P2X7R+/+
M1 P2X7R-/-
no ATP
time (min)
0
4
30
F
P2X7R-/- M1
LPS/IFNγ:
E. coli:
ATP:
Cells
proIL-1β
Media
mature IL-1β

Figure 3

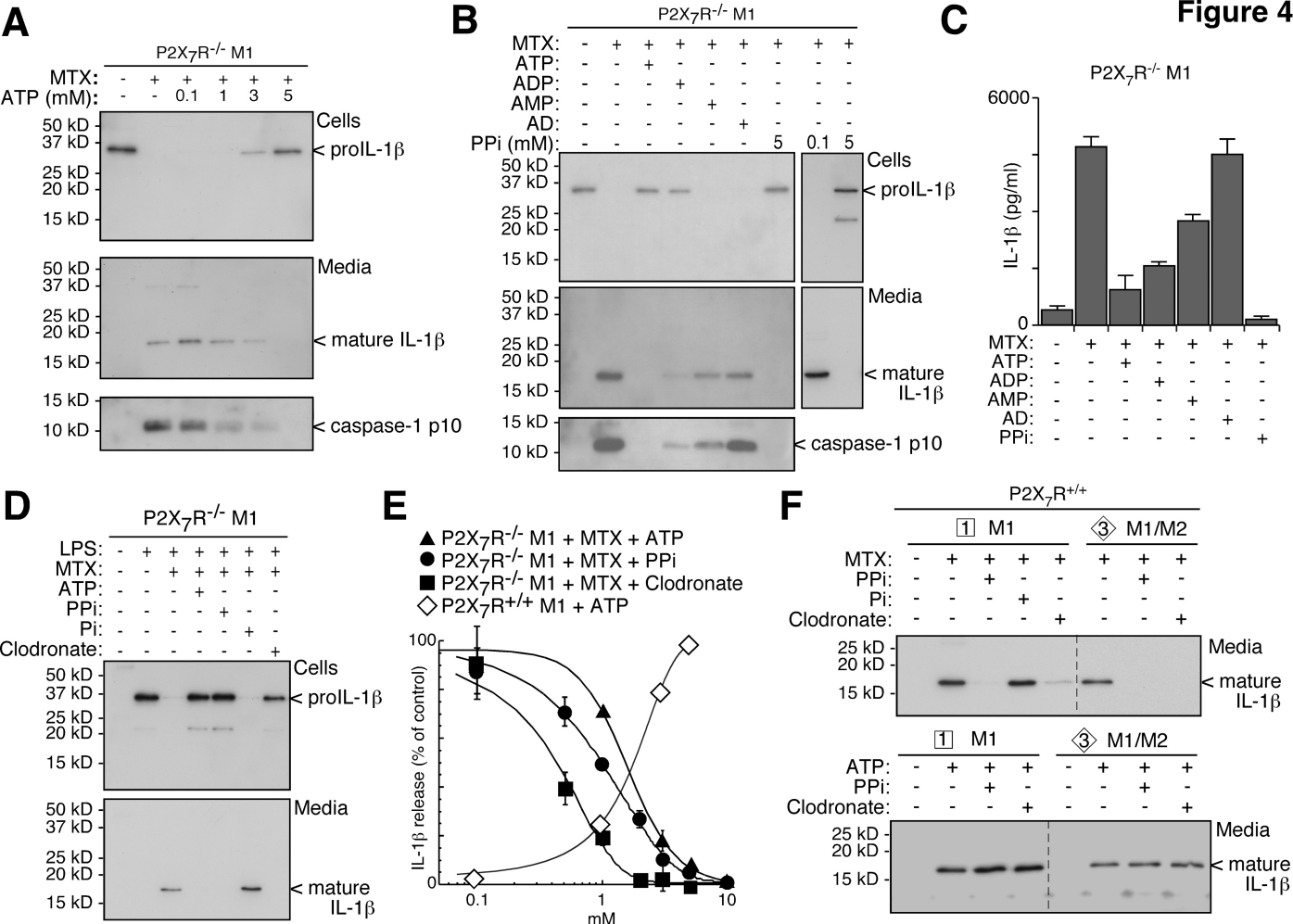
A
P2X7R-/- M1
MTX: - + + + + +
ATP (mM): - - 0.1 1 3 5
50 kD
37 kD
25 kD
20 kD
15 kD
Cells
< proIL-1β
Media
< mature IL-1β
15 kD
10 kD
< caspase-1 p10
B
P2X7R-/- M1
MTX: - + + + + + + + +
ATP: - - + - - - - - -
ADP: - - - + - - - - -
AMP: - - - - + - - - -
AD: - - - - - + - - -
PPi (mM): - - - - - - 5 0.1 5
Cells
< proIL-1β
Media
< mature IL-1β
< caspase-1 p10
C
P2X7R-/- M1
6000
0
IL-1β (pg/ml)
MTX: - + + + + + +
ATP: - + - - - - -
ADP: - - + - - - -
AMP: - - - + - - -
AD: - - - - + - -
PPi: - - - - - + +
D
P2X7R-/- M1
LPS: - + + + + + +
MTX: - - + + + + +
ATP: - - - + - - -
PPi: - - - - + - -
Pi: - - - - - + -
Clodronate: - - - - - - +
Cells
< proIL-1β
Media
< mature IL-1β
E
▲ P2X7R-/- M1 + MTX + ATP
● P2X7R-/- M1 + MTX + PPi
■ P2X7R-/- M1 + MTX + Clodronate
◇ P2X7R+/+ M1 + ATP
100
0
IL-1β release (% of control)
0.1
1
10
mM
F
P2X7R+/+
1 M1
3 M1/M2
MTX: - + + + + + + +
PPi: - - + - - - + -
Pi: - - - + - - - -
Clodronate: - - - - + - - +
Media
< mature IL-1β
ATP: - + + + - + + +
PPi: - - + - - + - -
Clodronate: - - - + - - - +

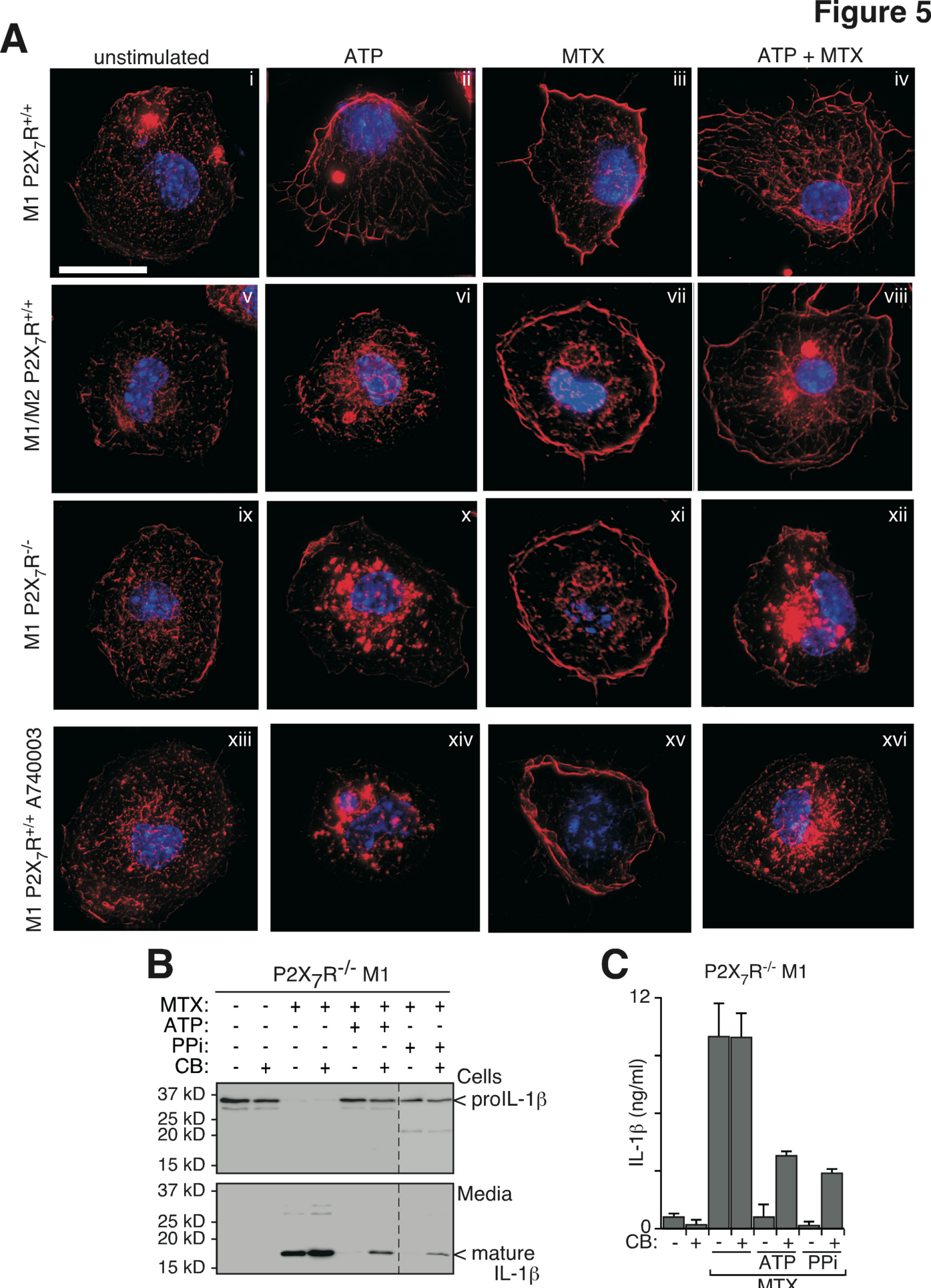
A
unstimulated
ATP
MTX
ATP + MTX
M1 P2X7R+/+
M1/M2 P2X7R+/+
M1 P2X7R-/-
M1 P2X7R+/+ A740003
i
ii
iii
iv
v
vi
vii
viii
ix
x
xi
xii
xiii
xiv
xv
xvi
B
P2X7R-/- M1
MTX: - - + + + + + +
ATP: - - - - + + - -
PPi: - - - - - - + +
CB: - + - + - + - +
Cells
37 kD
25 kD
20 kD
15 kD
< proIL-1β
Media
37 kD
25 kD
20 kD
15 kD
< mature IL-1β
C
P2X7R-/- M1
IL-1β (ng/ml)
12
0
CB: - + - + - + - +
ATP
PPi
MTX

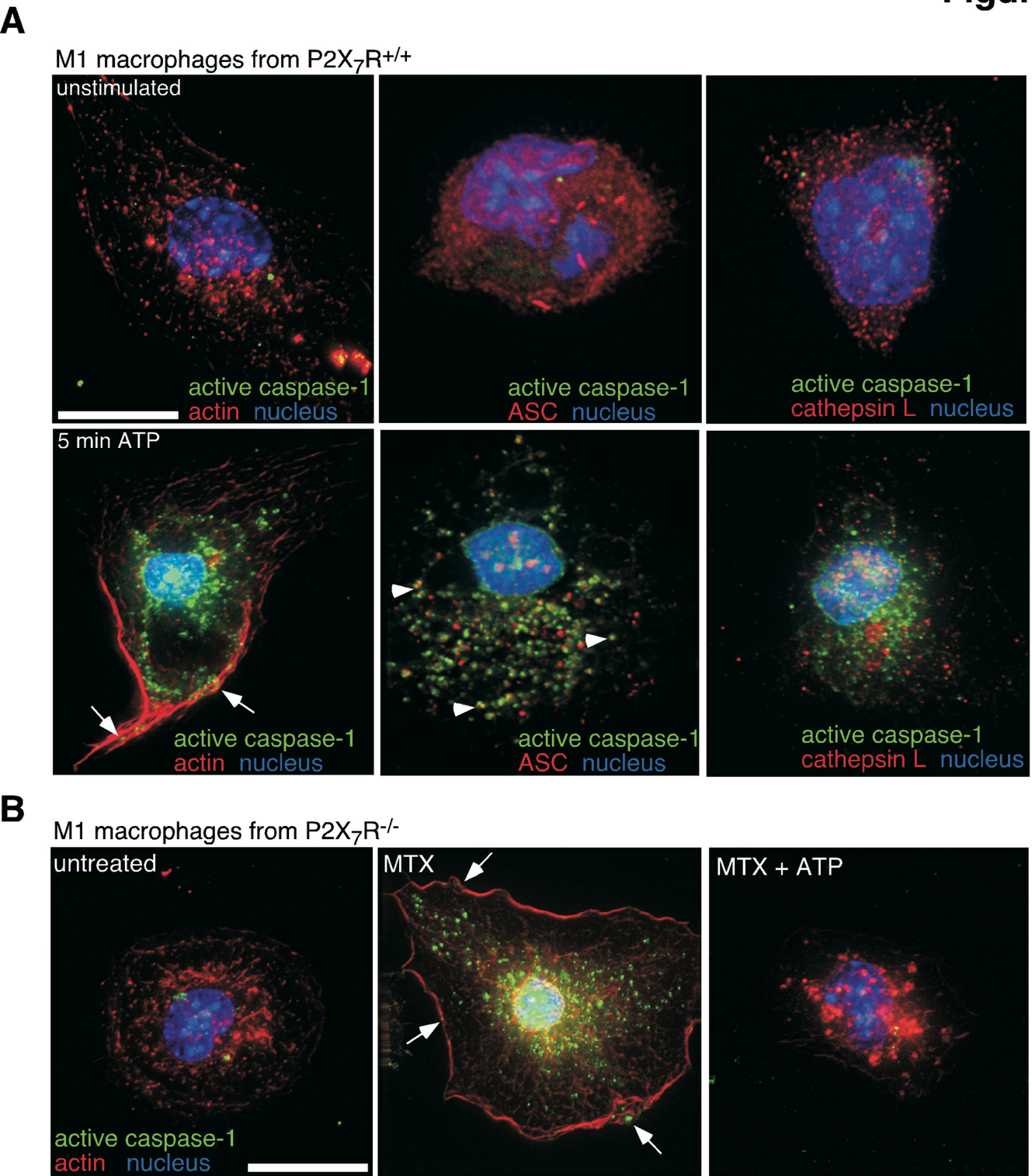
A
M1 macrophages from P2X7R+/+
unstimulated
active caspase-1
actin nucleus
active caspase-1
ASC nucleus
active caspase-1
cathepsin L nucleus
5 min ATP
active caspase-1
actin nucleus
active caspase-1
ASC nucleus
active caspase-1
cathepsin L nucleus
B
M1 macrophages from P2X7R-/-
untreated
active caspase-1
actin nucleus
MTX
MTX + ATP

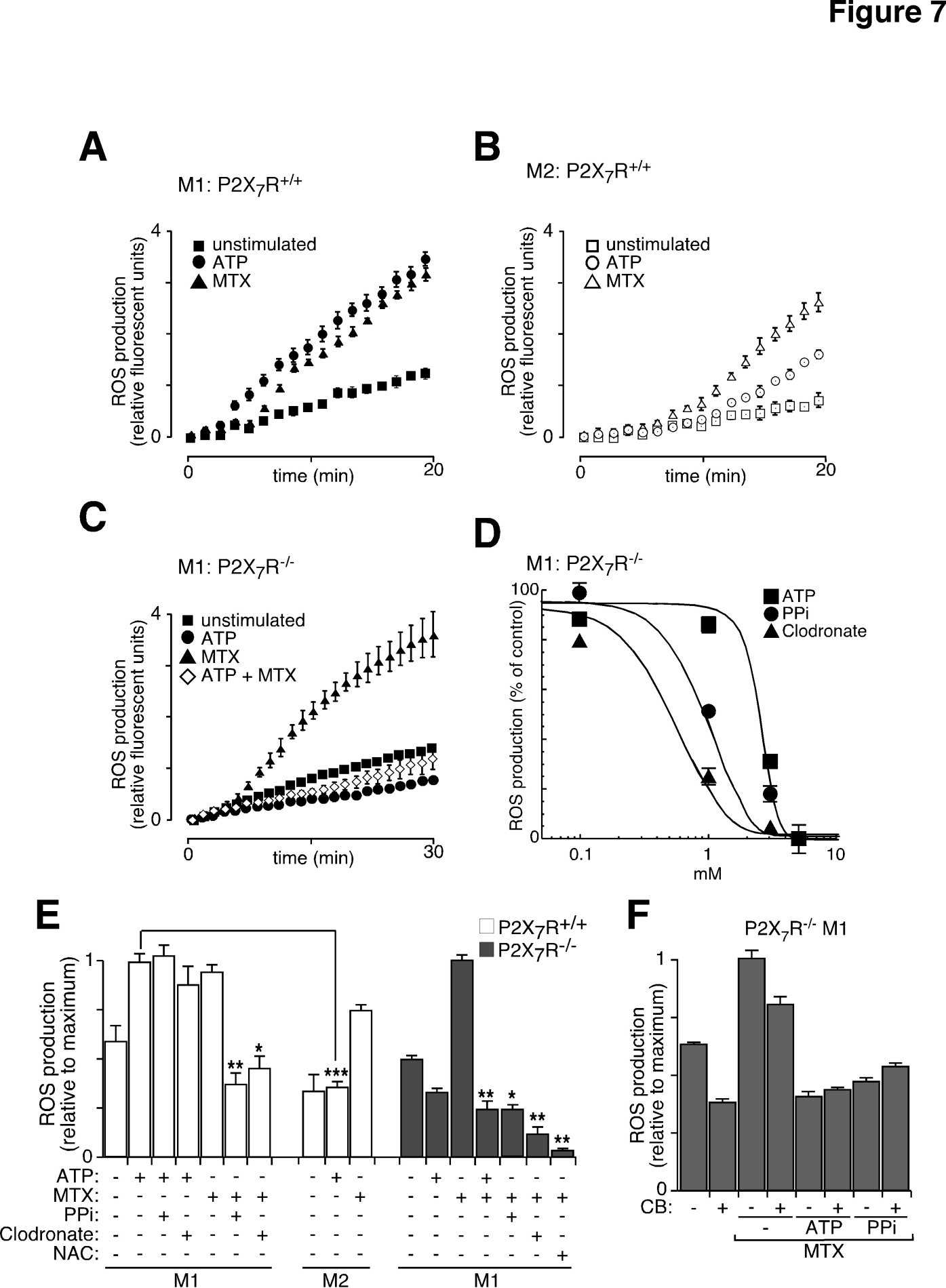
A
M1: P2X7R+/+
unstimulated
ATP
MTX
ROS production (relative fluorescent units)
time (min)
B
M2: P2X7R+/+
C
M1: P2X7R-/-
ATP + MTX
D
M1: P2X7R-/-
PPi
Clodronate
ROS production (% of control)
mM
E
P2X7R+/+
P2X7R-/-
ROS production (relative to maximum)
ATP:
MTX:
PPi:
Clodronate:
NAC:
M1
M2
M1
F
P2X7R-/- M1
CB:
ATP
PPi
MTX

Figure 8

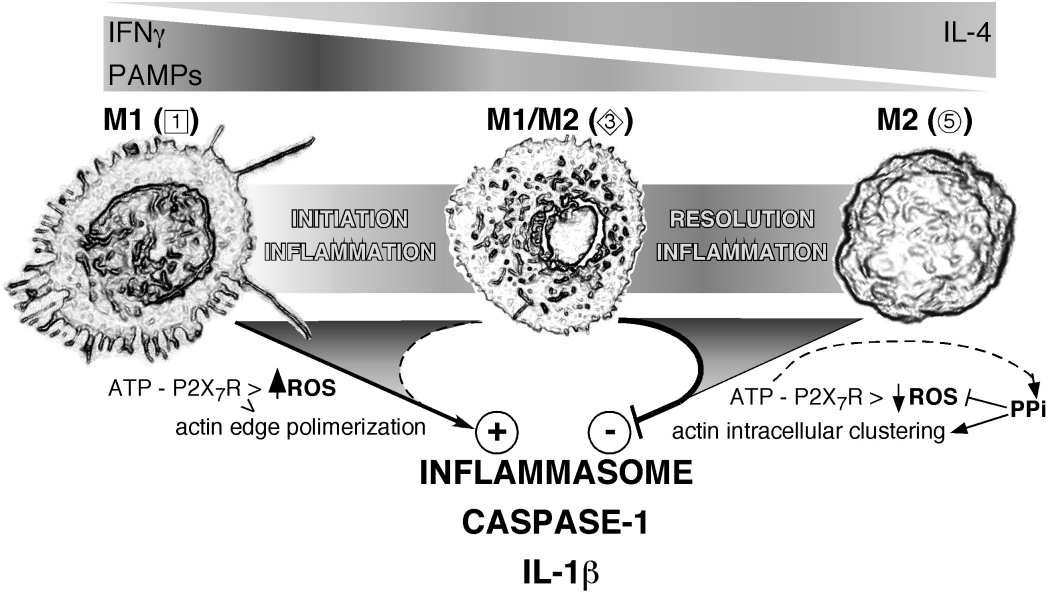
IFNγ
PAMPs
IL-4
M1 (1)
M1/M2 (3)
M2 (5)
INITIATION INFLAMMATION
RESOLUTION INFLAMMATION
ATP - P2X7R > ROS
actin edge polimerization
+
-
ATP - P2X7R > ROS
PPi
actin intracellular clustering
INFLAMMASOME
CASPASE-1
IL-1β

SUPPLEMENTAL FIGURE LEGENDS

Figure S1. **$P2X_7R$ mediates ATP induced IL-1β release but is not necessary for *E. coli*, maitotoxin or nigericin induced IL-1β release.** (A) Macrophage gradient polarization protocol used in this study. Five different stimulation conditions were used to establish a gradient between M1 and M2 extreme polarities, each one is identified by a number, a color and a shape trough the figures and the text to easily identify them. Fully M1 polarized macrophages (polarity state 1, square, red) were achieved by 4 h stimulation with LPS (1 μg/ml) and IFNγ (20 ng/ml); To achieve an intermediate macropahge polarity state close to M1, cells were stimulated first for 4 h with IL-4, washed and then stimulated for further 4 h with LPS/IFNγ (polarity state 2, star, pink); A combination of LPS/IFNγ/IL-4 for 4 h was used to differentiate a M1/M2 intermediate macrophage polarization phenotype (polarity state 3, diamond, green); Macrophages in a polarity close to M2 was achieve by stimulating first for 4 h with LPS/IFNγ, washed and then stimulated for further 4 h with IL-4 (20 ng/ml) (polarity state 4, triangle, yellow); IL-4 (20 ng/ml) was used for 4 h to differentiate to M2 phenotype (polarity state 5, round, blue). (B and C) Immunoblots for intracellular IL-1β (top panels) or released IL-1β (bottom panels) in M1 polarized (1: LPS and IFNγ) peritoneal macrophages from wild type ($P2X_7R^{+/+}$) or $P2X_7R$-deficient ($P2X_7R^{-/-}$) mice stimulated for 15 min with ATP (5 mM) (B,C), maitotoxin (MTX, 0.2 nM) or nigericin (5 μM) (B) or *E. coli* (4 h) (C). (D) Immunoblots for intracellular IL-1β (top panel) or released IL-1β (bottom panel) in peritoneal macrophages from wild type ($P2X_7R^{+/+}$) or $P2X_7R$-deficient ($P2X_7R^{-/-}$) mice infected for 48 h with an empty adenovirus or with a $P2X_7R$-adenovirus construct following polarization to M1 and stimulated for 15 min with ATP (5 mM). (E) ELISA for released IL-1β (top panel) or immunoblots for released active caspase-1 (p10 subunit, bottom panel) in peritoneal macrophages from $P2X_7R$-deficient mice ($P2X_7R^{-/-}$) infected for 48 h with a $P2X_7R$-adenovirus construct following polarization to M1 and stimulated for 15 min with ATP (5 mM), MTX (0.2 nM) or a combination of ATP and MTX; n = 3 independent cultures for ELISA and blots are representative of 2 independent experiments.

Figure S2. **Negative regulation of NLRP3 inflammasome by ATP.** (A) IL-1β release by M1 polarized (1: LPS and IFNγ) or intermediate polarized (3: LPS, IFNγ

and IL-4) mouse peritoneal macrophages activated for 15 min with ATP (5 mM), maitotoxin (MTX, 0.2 nM) or a combination of ATP and MTX detected by immunoblot; blots are representative of 3 independent experiments. (B) IL-1β release by M1 polarized mouse peritoneal macrophages induced by 15 min of ATP (5 mM), MTX (0.2 nM) or a combination of ATP and MTX in the presence of absence of $P2X_7R$ antagonist A740003 (10 μM, 5 min before ATP/MTX) detected by ELISA; *n* = 3 independent cultures for ELISA; $^{\#}p=0.0027$; $^{\#\#}p=3.5x10^{-5}$. (C) Densitometry quantification of immunoblots for the release of mature IL-1β relative to the maximum release from M1 polarized or state 3 intermediate polarized peritoneal macrophages from wild type ($P2X_7R^{+/+}$) or $P2X_7R$-deficient ($P2X_7R^{-/-}$) mice stimulated for 15 min with ATP (5 mM), maitotoxin (MTX, 0.2 nM), nigericin (5 μM) or a combination of ATP and MTX or ATP and nigericin (*n* values are shown in parentheses above each bar and correspond to independent experiments); *p=0.0093; **p=0.0005; ***p=0.0003; $^{\#}p=1.7x10^{-6}$. (D) $P2X_7R^{-/-}$ murine M1 polarized peritoneal macrophages were challenged with *E. coli* for 1 h in the absence or presence of 5 mM ATP and further incubated for 4 h, IL-1β was detected by ELISA; *n* = 3 independent cultures for ELISA and representative from 3 independent experiments; *p=0.0042. (E) Phagocytosis of FITC-labeled *E. coli* in the absence or presence of 5 mM ATP by $P2X_7R^{-/-}$ murine M1 polarized peritoneal macrophages; solid bars represent binding and internalized (uptake) bacteria, open bars represent only internalized (uptake) bacteria after quenching extracellular fluorescent by 0.4 % trypan blue; *n* = 3 independent cultures.

Figure S3. **Negative regulation of IL-1β release by triphosphates.** (A) ELISA for released IL-1β induced by nigericin (NIG; 5 μM, 15 min) or a combination of NIG with 5 mM ATP in M1 polarized (1: LPS and IFNγ) peritoneal macrophages from $P2X_7R$-deficient mice ($P2X_7R^{-/-}$) in the presence or absence of suramin (50 μM) or Pyridoxal-phosphate-6-azophenyl-2',4'-disulfonate (PPADS; 50 μM) 5 min before NIG stimulation. (B) LDH release from peritoneal macrophages treated for 30 min with PPi (5 mM) or clodronate (1 mM); value represented as a percentage of total intracellular LDH averaged from 10 to 14 independent experiments. (C) ELISA for released IL-1β induced by MTX (0.2 nM, 15 min) in M1 polarized peritoneal macrophages from $P2X_7R^{-/-}$ mice in the presence or absence of 5 mM ATP or

triphosphate (PPP) (left panel) or in the presence of the indicated concentrations of PPP (right panel). (D) Chemical structure of ATP, PPi, clodronate and PPP. (E) Fura2 fluorescence ratio recorded from HEK293 cells stable expressing $P2X_2$ or $P2X_7$ receptors. PPi (5 mM) or clodronate (1 mM) were added when indicated and did not alter intracellular calcium levels. P2Y or P2X receptors were activated with ATP (1 mM) resulting in typical intracellular calcium increase. Traces are the average of 4 – 6 independent cultures and representative of 2 independent experiments.

Figure S4. **ATP, PPi and clodronate regulate actin polymerization**. (A and B) High-resolution, deconvolved images of F-actin cytoskeleton labeled with Texas Red-phalloidin in peritoneal macrophages isolated from $P2X_7R$-deficient mice ($P2X_7R^{-/-}$) after differentiation to M1 (1: LPS and IFNγ) and stimulated for 5 min with MTX (0.2 nM), ATP (5 mM) or a combination of MTX with 5 mM of ATP, PPi or clodronate in the absence (A) or presence of cytochalaisin B (CB; 2.5 μg/ml, 5 min before MTX) (B). MTX induces actin polymerization to the edge of the cell (arrowheads) and ATP, PPi or clodronate induce intracellular actin clustering (arrows) and prevents MTX induced actin edge polimerization. Bar, 5 μm. Images are representative of two independent experiments. (C) Discrete F-actin fluorescence quantification. 50 region of interest were defined inside of each cell around F-actin spots of fluorescence and 10 region of interest were defined around cell edge, integrated fluorescence density was calculated for intracellular or edge fluorescence multiplying the area of the region of interest with the mean fluorescence intensity. Presented is the average and standard error of the intracellular or edge integrated fluorescence density from 10 different cells unstimulated or treated for 5 min with MTX (0.2 nM) or a combination of MTX and 5 mM of ATP, PPi or 1 mM of clodronate. (D) Negative regulation of IL-1β release by antioxidants. ELISA for released IL-1β induced by MTX (0.2 nM, 15 min) in M1 polarized peritoneal macrophages from $P2X_7R^{-/-}$ mice in the presence or absence of 5 mM of ATP, 3 mM PPi, 20 mM N-acetyl cystein (NAC) or 10 μM α-tocopherol.

Figure S1

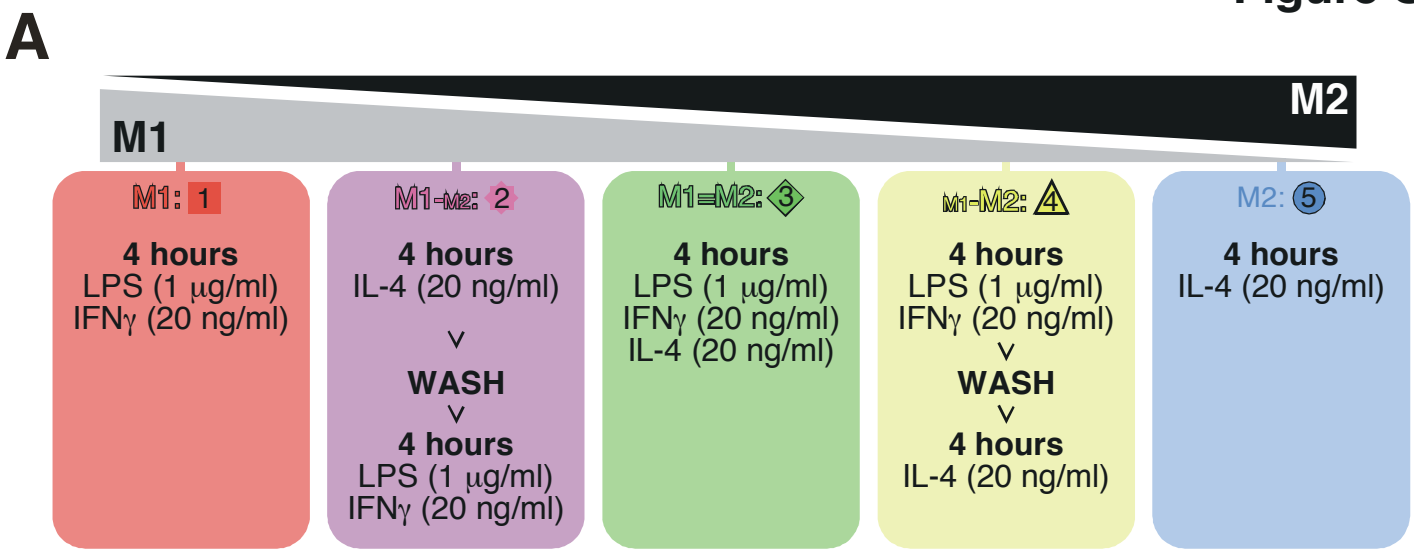
A
M1
M2
M1: 1
4 hours
LPS (1 μg/ml)
IFNγ (20 ng/ml)
M1-M2: 2
4 hours
IL-4 (20 ng/ml)
∨
WASH
∨
4 hours
LPS (1 μg/ml)
IFNγ (20 ng/ml)
M1=M2: 3
4 hours
LPS (1 μg/ml)
IFNγ (20 ng/ml)
IL-4 (20 ng/ml)
M1-M2: 4
4 hours
LPS (1 μg/ml)
IFNγ (20 ng/ml)
∨
WASH
∨
4 hours
IL-4 (20 ng/ml)
M2: 5
4 hours
IL-4 (20 ng/ml)

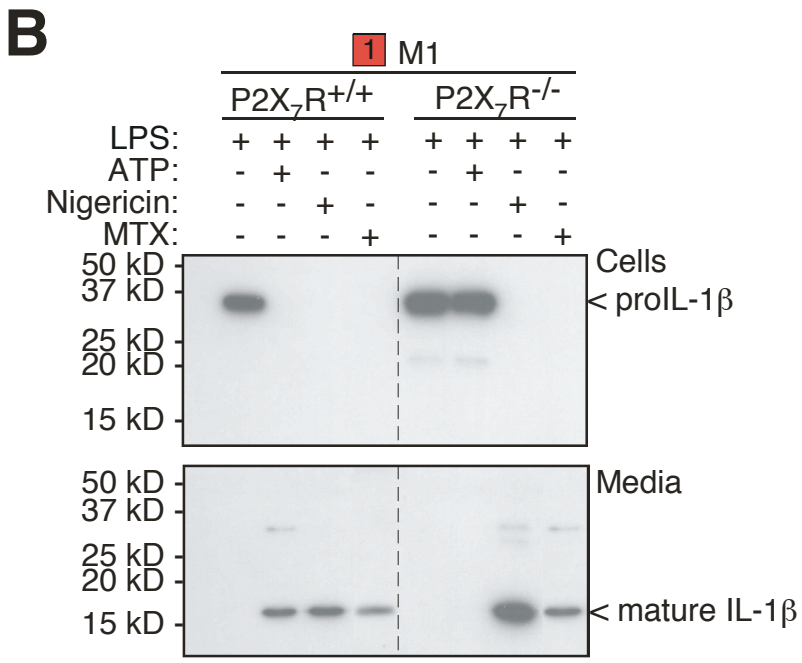
B
1 M1
P2X7R+/+
P2X7R-/-
LPS:
ATP:
Nigericin:
MTX:
50 kD
37 kD
25 kD
20 kD
15 kD
Cells
< proIL-1β
Media
< mature IL-1β

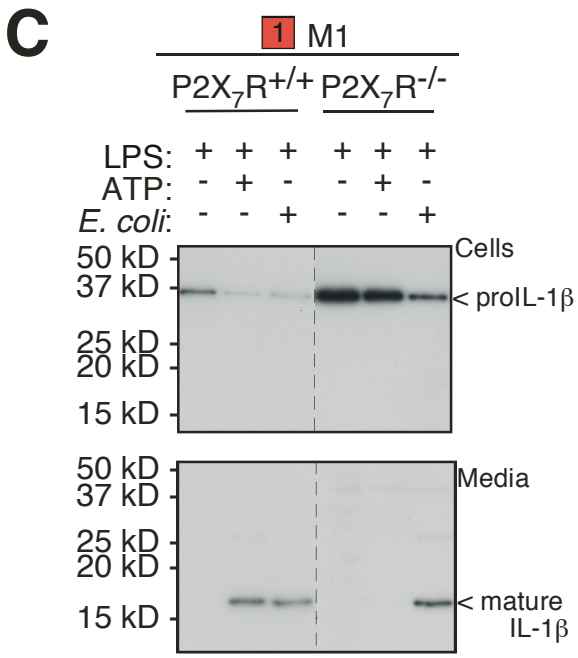
C
1 M1
P2X7R+/+
P2X7R-/-
LPS:
ATP:
E. coli:
50 kD
37 kD
25 kD
20 kD
15 kD
Cells
< proIL-1β
Media
< mature IL-1β

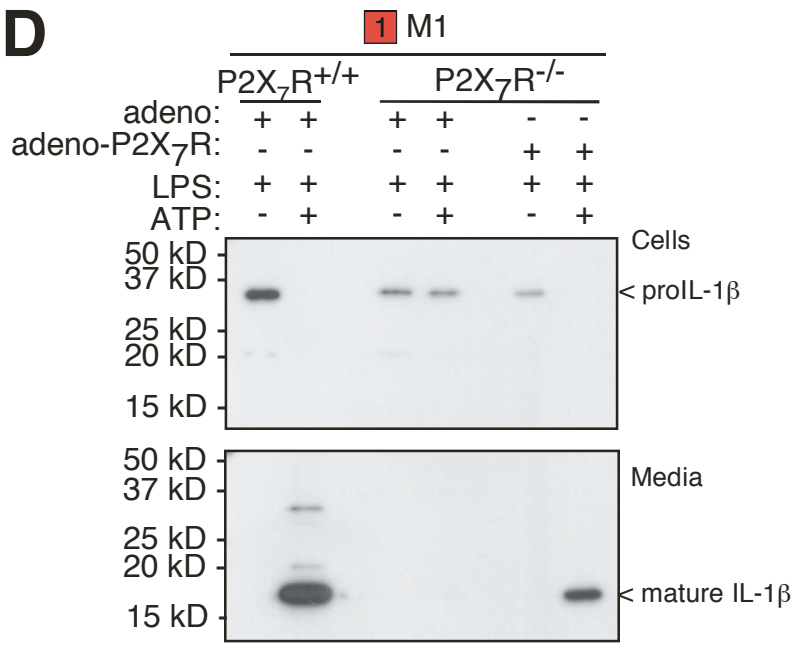
D
1 M1
P2X7R+/+
P2X7R-/-
adeno:
adeno-P2X7R:
LPS:
ATP:
50 kD
37 kD
25 kD
20 kD
15 kD
Cells
< proIL-1β
Media
< mature IL-1β

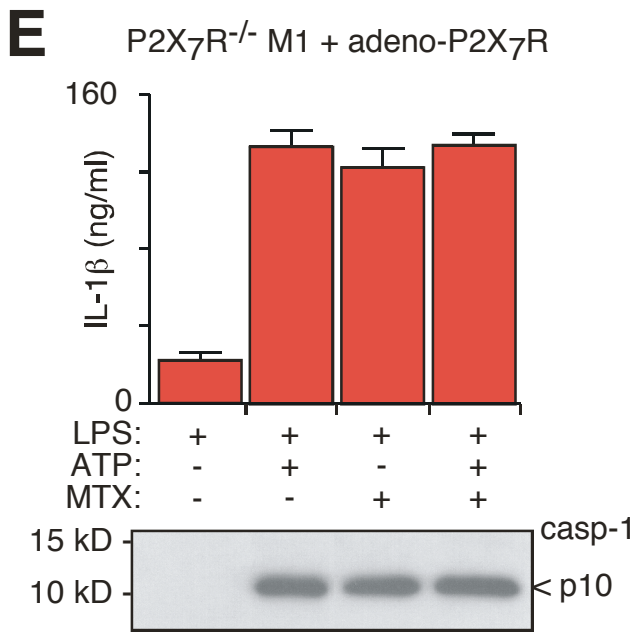
E
P2X7R-/- M1 + adeno-P2X7R
160
IL-1β (ng/ml)
0
LPS:
ATP:
MTX:
15 kD
10 kD
casp-1
< p10

Figure S2

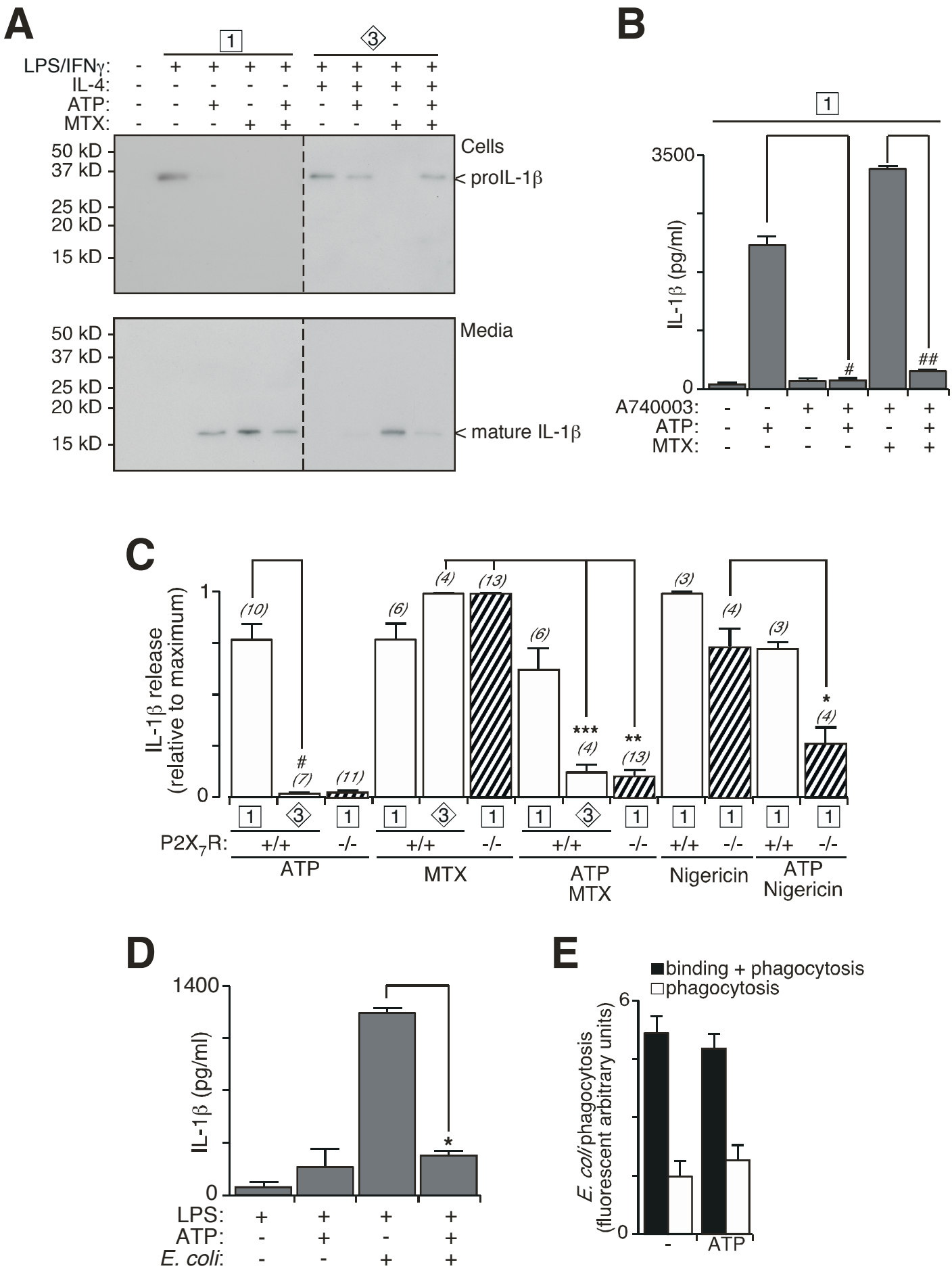
A
1
3
LPS/IFNγ: - + + + + + + + +
IL-4: - - - - - + + + +
ATP: - - + - + - + - +
MTX: - - - + + - - + +
50 kD
37 kD
25 kD
20 kD
15 kD
Cells
< proIL-1β
Media
< mature IL-1β
B
1
3500
0
IL-1β (pg/ml)
#
##
A740003: - - + + + +
ATP: - + - + - +
MTX: - - - - + +
C
IL-1β release (relative to maximum)
1
0
(10)
#
(7)
(11)
(6)
(4)
(13)
(6)
***
(4)
**
(13)
(3)
(4)
(3)
*
(4)
P2X7R: +/+ -/- +/+ -/- +/+ -/- +/+ -/- +/+ -/- +/+ -/-
ATP
MTX
ATP MTX
Nigericin
ATP Nigericin
D
1400
0
IL-1β (pg/ml)
*
LPS: + + + +
ATP: - + - +
E. coli: - - + +
E
binding + phagocytosis
phagocytosis
6
0
E. coli phagocytosis (fluorescent arbitrary units)
-
ATP

Figure S3

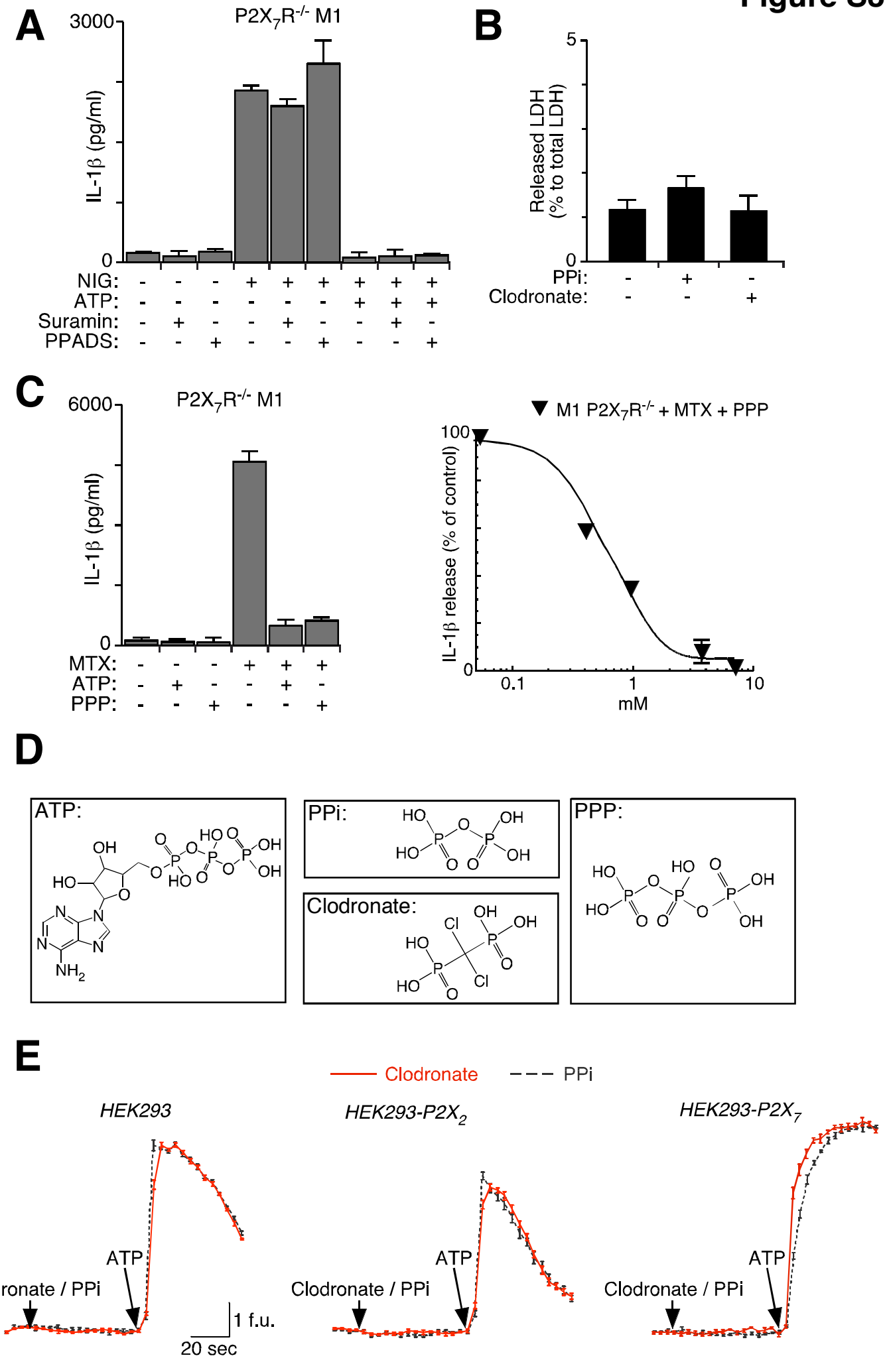
A
P2X7R-/- M1
IL-1β (pg/ml)
3000
0
NIG:
ATP:
Suramin:
PPADS:
B
Released LDH (% to total LDH)
5
0
PPi:
Clodronate:
C
P2X7R-/- M1
IL-1β (pg/ml)
6000
0
MTX:
ATP:
PPP:
M1 P2X7R-/- + MTX + PPP
IL-1β release (% of control)
100
0
0.1
1
10
mM
D
ATP:
PPi:
Clodronate:
PPP:
E
Clodronate
PPi
HEK293
HEK293-P2X2
HEK293-P2X7
ATP
Clodronate / PPi
1 f.u.
20 sec

Figure S4

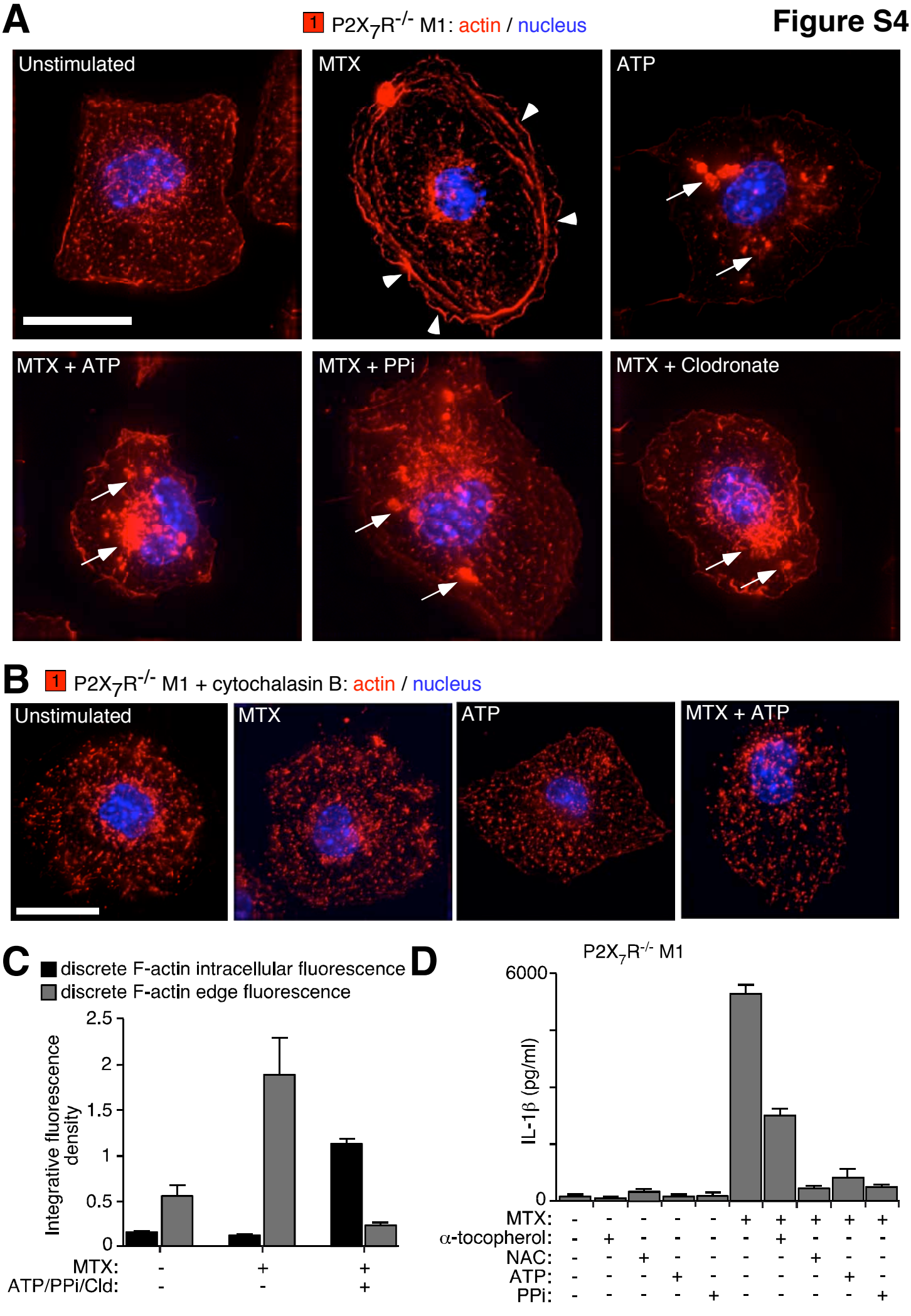
A
1 P2X7R-/- M1: actin / nucleus
Unstimulated
MTX
ATP
MTX + ATP
MTX + PPi
MTX + Clodronate
B
1 P2X7R-/- M1 + cytochalasin B: actin / nucleus
Unstimulated
MTX
ATP
MTX + ATP
C
discrete F-actin intracellular fluorescence
discrete F-actin edge fluorescence
Integrative fluorescence density
2.5
2
1.5
1
0.5
0
MTX: - + +
ATP/PPi/Cld: - - +
D
P2X7R-/- M1
IL-1β (pg/ml)
6000
0
MTX: - - - - - + + + + +
α-tocopherol: - + - - - - + - - -
NAC: - - + - - - - + - -
ATP: - - - + - - - - + -
PPi: - - - - + - - - - +

SUPPLEMENTAL METHODS

Phagocytosis assay

Bacteria were grown overnight at 37ºC under shaking in LB broth. Bacteria were diluted 1/50 and cultured for further 2 h, then washed and killed with 4% formaldehyde in PBS for 30 min at room temperature, washed and labeled with FITC (Sigma) at 500 μg/ml in PBS for 30 min at room temperature and aliquots were stored in PBS at -80ºC. Peritoneal macrophages isolated from $P2X_7R$-deficient mice ($P2X_7R^{-/-}$) were plated in 96-well plate black with clear bottom, stimulated with LPS and IFNγ for 2 h and mixed with FITC-labeled *E. coli* in the presence or absence of 5 mM ATP for 4 h. After this incubation period each well was washed three times with PBS to remove the non-bound non-internalized bacteria. The green fluorescence of the FITC-labeled *E. coli* was measured using FlexStation 3 with the excitation set to 492 nm and the emission to 520 nm, and represents the association (binding and internalization) of *E. coli* with the macrophages. Supernatant was removed and 100 μl of 0.4 % Trypan Blue (Sigma) in E-total was added for 2 min and washed away to quench the FITC-labeled *E. coli* that had not been ingested by the phagocytes. The plate was read again to measure the bacteria that had been taken up by the adherent phagocytes. All experiments were performed in quadruplicates and repeated three times.

LDH release assay

The presence of LDH in the media was measured using the Cytotoxicity Detection kit (Roche) following manufacturer instructions and expressed as percent of the total amount of LDH in the cells. Average results from triplicate samples are expressed as the mean ± s.e.m. from 10 to 14 independent experiments per condition.